Geoscience Frontiers 14 (2023) 101515

HOSTED BY

Contents lists available at ScienceDirect

Geoscience Frontiers

journal homepage: www.elsevier.com/locate/gsf

Research Paper

Unravelling the protracted U-Pb zircon geochronological record of high to ultrahigh temperature metamorphic rocks: Implications for provenance investigations

Mahyra Tedeschi [a,b,*], Pedro Leonardo Rossi Vieira [a], Matheus Kuchenbecker [c], Bruno V. Ribeiro [d,e], Vitor Barrote [f], Humberto Reis [g], Laura Stutenbecker [h], Cristiano Lana [g], Antonio Pedrosa-Soares [a], Ivo Dussin [i]

[a] Programa de Pós-graduação em Geologia da Universidade Federal de Minerais, Centro de Pesquisas Manoel Teixeira da Costa, Institute of Geosciences, Federal University of Minas Gerais, Av. Antônio Carlos, 6627, Belo Horizonte 31270-901, Brazil
[b] Institute of Geological Sciences, University of Bern, 3012 Bern, Switzerland
[c] Laboratório de Estudos Tectônicos, Universidade Federal dos Vales do Jequitinhonha e Mucuri, Rodovia MGT 367, Km 583–Diamantina 39100-000, Brazil
[d] School of Earth, Atmosphere and Environment, Monash University, Clayton, Victoria 3800, Australia
[e] Timescales of Mineral Systems Group, School of Earth and Planetary Sciences, Curtin University, Perth, WA 6845, Australia
[f] Freie Universität Berlin, Institut für Geologische Wissenschaften, Geochemie, Malteserstr. 10 74-100, 12249 Berlin, Germany
[g] Departamento de Geologia-Escola de Minas, Universidade Federal de Ouro Preto 35400-000, Brazil
[h] Department of Materials and Earth Sciences, Institute of Applied Geosciences, TU Darmstadt, Schnittspahnstr. 9, 64287 Darmstadt, Germany
[i] TEKTOS Geotectonic Research Group, Geology Institute, Rio de Janeiro State University, São Francisco Xavier Street, 524/4030-A, Maracanã, Rio de Janeiro 20550-900, Brazil

ARTICLE INFO

Article history:
Received 7 February 2022
Revised 18 October 2022
Accepted 20 November 2022
Available online 24 November 2022
Handling Editor: Nick Roberts

Keywords:
Detrital zircon
Protracted zircon record
Sedimentary basins
UHT metamorphism
Prolonged metamorphism
Bias in detrital zircon

ABSTRACT

The assessment of detrital zircon age records is a key method in basin analysis, but it is prone to several biases that may compromise accurate sedimentary provenance investigations. High to ultrahigh temperature (HT-UHT) metamorphism (especially if $T > 850$ °C) is herein presented as a natural cause of bias in provenance studies based on U-Pb detrital zircon ages, since zircon from rocks submitted to these extreme and often prolonged conditions frequently yield protracted, apparently concordant, geochronological records. Such age spreading can result from disturbance of the primary U-Pb zircon system, likewise from (re)crystallization processes during multiple and/or prolonged metamorphic events. In this contribution, available geochronological data on Archean, Neoproterozoic and Palaeozoic HT-UHT metamorphic rocks, acquired by different techniques (SIMS and LA-ICP-MS) and showing distinct compositions, are reassessed to demonstrate HT-UHT metamorphism may result in modes and age distributions of unclear geological meaning. As a consequence, it may induce misinterpretations on U-Pb detrital zircon provenance analyses, particularly in sedimentary rocks metamorphosed under such extreme temperature conditions. To evaluate the presence of HT-UHT metamorphism-related bias in the detrital zircon record, we suggest a workflow for data acquisition and interpretation, combining a multi-proxy approach with: (i) *in situ* U-Pb dating coupled with Hf analyses to retrieve the isotopic composition of the sources, and (ii) the integration of a petrochronological investigation to typify fingerprints of the HT-UHT metamorphic event. The proposed workflow is validated in the investigation of one theoretical and one natural example allowing a better characterization of the sedimentary sources, maximum depositional ages, and the tectonic setting of the basin. Our workflow allows to the appraisal of biases imposed by HT-UHT metamorphism and resulting disturbances in the U-Pb detrital zircon record, particularly for sedimentary rocks that underwent HT-UHT metamorphism and, finally, suggests ways to overcome these issues.

* Corresponding author at: Programa de Pós-graduação em Geologia da Universidade Federal de Minerais, Centro de Pesquisas Manoel Teixeira da Costa, Institute of Geosciences, Federal University of Minas Gerais, Brazil.
E-mail address: mtedeschi@ufmg.br (M. Tedeschi).

https://doi.org/10.1016/j.gsf.2022.101515

1. Introduction

The investigation of crustal evolution has long been the focus of many studies in different branches of the Earth Sciences. Numerous advances in the last decades have contributed to improve the understanding of how continental crust is generated and recycled through geological time (e.g., Cawood et al., 2012; Hastie et al., 2016; Johnson et al., 2017; Pereira et al., 2021). Detrital zircon grains extracted from sedimentary or metasedimentary rocks play an important role in assembling the puzzle of continental crust evolution. The detrital zircon record registers different aspects of the formation and distribution of multiple sedimentary sources, sometimes no longer preserved or exposed. Therefore, they represent important physical remnants to assess the conditions and rates under which the continental crust evolved through the geological time (Cawood et al., 2013; Andersen et al., 2019; Barham et al., 2019). U-Pb dating of detrital zircon has been key to investigate crustal processes, revealing the maximum depositional ages (MDA) of sedimentary successions where absolute dating of *syn*-sedimentary volcanic rocks is not possible (e.g., Nelson, 2001; Coutts et al., 2019). Furthermore, detrital zircon dating is used to match crystallization ages and patterns of protosource rocks, often combined with isotopic and elemental chemistry (e.g., Fedo et al., 2003; Andersen, 2005; Litty et al., 2017). Analysing the age distributions of detrital zircon ages has been considered an effective tool in assessing the tectonic setting of ancient sedimentary basins, since different tectonic environments may affect the evolution of sedimentary basins, inducing distinct sediment dispersal (Cawood et al., 2012). These analyses are key in paleogeographic and palaeotectonic reconstructions (Murphy et al., 2004) and in improving the understanding of continental crustal growth (Belousova et al., 2010; Chowdhury et al., 2021; Mulder et al., 2021).

Analytical advances in U-Pb geochronology improved strategies in statistical analysis of data (Spencer et al., 2016) and "the assumption of qualitative representativity" (cf., Andersen et al., 2019) promoted progress in the systematics of detrital zircon investigations. Nonetheless, several natural and artificial processes that could bias provenance interpretations still interfere in modern detrital zircon studies. Possible biases include differential zircon fertility, selective preservation of rocks (e.g., Cawood et al., 2013; Schoene, 2014) and different mineral separation strategies (Dröllner et al., 2021). In this scenario, metamorphism has been recognized as a potential source of natural bias, since regional and contact metamorphism can play a role in inducing post-depositional Pb loss and partial recrystallization of zircon (Andersen et al., 2019 and references therein), affecting the U-Pb geochronometer.

The effect introduced by high to ultrahigh temperature (UHT) metamorphism, however, remains overlooked despite its disruptive effects on detrital zircon age distributions (e.g., Chew et al., 2020). Rocks that have experienced temperatures higher than 900 °C (UHT stricto sensu), and in some cases 850 °C (high-temperature; HT), often exhibit a continuous spectrum of concordant to slightly discordant U-Pb dates (i.e., a protracted record), which could be the result of concealed Pb-loss, partial recrystallization, dissolution-reprecipitation and/or diffusion or annealing, and mixed analyses of domains (Friend and Kinny, 1995; Lee et al., 1997; Wan et al., 2011; Bindeman and Melnik, 2016; Andersen et al., 2019). Despite covering a relatively small surface of the globe, HT and UHT metamorphic rocks have widespread distribution. More than 58 occurrences of UHT metamorphism (Kelsey and Hand, 2015) have been identified around the world in rocks as old as the Paleoarchean, mainly associated with back-arc basins, ridge subduction and continent–continent collisional settings (Harley, 2016; Santosh and Kusky, 2010), and less commonly, to contact metamorphism (Wisniowski et al., 2021). Furthermore, spreading of U-Pb zircon dates has also been reported in rocks metamorphosed at HT such as around 850 °C (Kunz et al., 2018), increasing the potential for this bias to impact the detrital zircon record of sedimentary basins worldwide.

In this study, we explore the different processes taking place during HT-UHT metamorphism which can produce protracted U-Pb zircon records and present a strategy to decode this record, focusing on high-grade metamorphic rocks, to extract more accurate zircon ages that may contribute to provenance investigations. We employ two examples, one theoretical and one natural of metasedimentary rock records to demonstrate that HT-UHT metamorphism might introduce bias in zircon provenance investigations. Finally, we discuss the effect of the protracted record in detrital zircon investigations of high-grade metamorphic rocks and their unfolding to non-metamorphosed sedimentary rocks and propose a flowchart with a workflow to guide the identification and an approach to mitigate HT-UHT metamorphism induced bias.

2. Background

2.1. Zircon U-Pb systematics

Zircon has been a fundamental mineral to resolve many geological problems given its ability to precisely date a diverse range of geological processes that shed light into sedimentary provenance (Paula-Santos et al., 2015; Moreira et al., 2016; Kuchenbecker et al., 2020; Seraine et al., 2021), igneous (Araujo et al., 2020; Ribeiro et al., 2020) and metamorphic events (Rubatto, 2002; Ganade de Araujo et al., 2014). However, zircon U-Pb systematic can be affected, among several reasons, by HT-UHT metamorphism hampering the analysis of geological evolution. Zircon U-Pb data from HT-UHT migmatite and granulite rocks have revealed that concordant to slightly concordant dates spectra spreading over several million years is relatively common (e.g., Whitehouse and Kemp, 2010; Fornelli et al., 2011; Laurent et al., 2018; Rocha et al., 2018; Taylor et al., 2020). This spreading might be related to processes such as (i) episodic zircon growth likely associated with partial resetting between distinct thermal events, (ii) long-lived partial melting events, and (iii) post-crystallization disturbance of the U-Pb isotopic system (Corfu et al., 2003; Taylor et al., 2016; Rubatto, 2017) and (iv) analytical effect, resulting by the mixing of (micro) domains of distinct isotopic composition (e.g., Whitehouse et al., 2014). In the present work, therefore, the term 'date' is employed in referring to an individual U-Pb zircon number obtained from isotopic ratios of spot analysis, and the term 'age' is used for pooled dates for which geological significance is assigned (Schoene et al., 2013; Horstwood et al., 2016; Kunz et al., 2018).

2.1.1. Post-crystallization disturbance of zircon U-Pb system

Changes in the zircon composition and internal texture without external shape modification represents the most common type of disturbance to the zircon chemistry (e.g., annealing, metamictization). Hence, zircon crystals of a *meta*-igneous rock may preserve their primary texture even after affected by post crystallization processes (Fig. 1; Corfu et al., 2003). Zircon grains subjected to HT-UHT metamorphism often present scattered inner U-Pb dates (Fig. 1B; Tedeschi et al., 2018) commonly with cores younger than the rims (i.e., inverse-age zoning; Laurent et al., 2018; Costa et al., 2022). Such grains often remain concordant (to slightly discordant) and do not necessarily present clear evidence of Pb loss. Radiation damage recovery during metamorphism (annealing) is described by Laurent et al. (2018) as the process responsible for partial

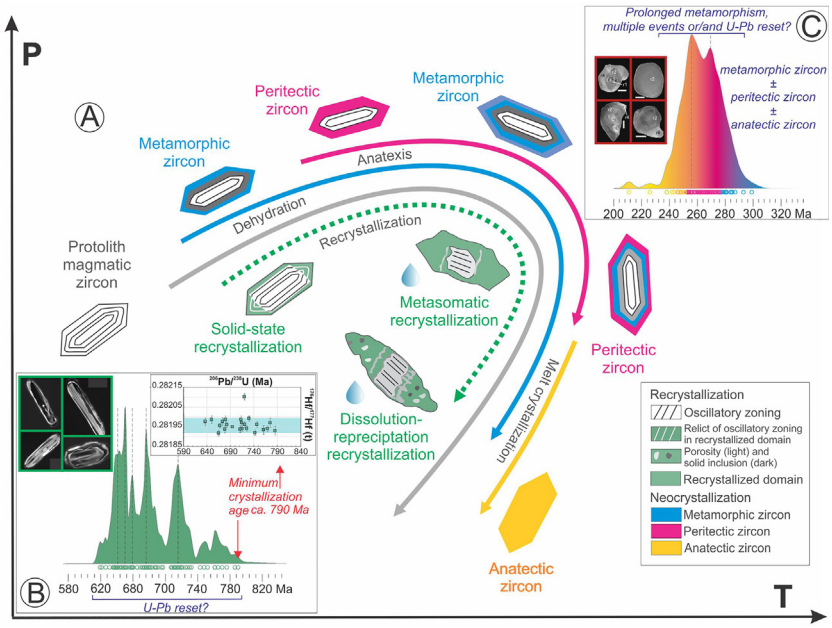

Fig. 1. Schematic cartoon summarising potential zircon formation and recrystallization events during metamorphism (grey trajectory), the respective resulting zircon textures visible in cathodoluminescence images, and their U-Pb zircon record in probability density plots. (A) Growth of zircon under different pressure, temperature, and fluid conditions. Zircon recrystallization can occur along the whole pressure–temperature path, strongly controlled by the availability of fluids. Fluid-absent systems result in solid-state recrystallization, while metasomatic and dissolution recrystallization occur in the presence of fluid (adapted from Chen and Zheng, 2017; the blue path for subsolidus, pink for peritectic, and yellow for anatectic reactions in A). (B) Zircon $^{206}Pb/^{238}U$ date spectrum of a single Neoproterozoic metamorphosed igneous rock exhibiting a protracted record of concordant grains with partial preservation of igneous textures and Hf isotopic signatures. Besides the presence of several dates modes lacking geological meaning (dashed vertical lines) the rock has only one geological meaningful age of ca. 790 Ma, interpreted as the minimum crystallization age. The protracted record is attributed to post-crystallization U-Pb disturbance (recrystallization, corresponding to the green path in A; Metaopdalite C8382 from Tedeschi et al., 2018). (C) Zircon $^{206}Pb/^{238}U$ date spectrum of zircon with metamorphic textures from a Cambrian migmatite (Paragneiss IZ-405 from Kunz et al., 2018) showing a protracted record with two dates modes. The spreading of U-Pb data from Kunz et al. (2018) is herewith interpreted as likely representing one or more mechanisms of resetting and neocrystallization (the coloured areas and circles through the detrital zircon spectrum represent the predominance of each of the processes from A in a neocrystallization scenario).

resetting of the U-Pb system in zircon cores, and it is dependent of distinct variables such as the size of the grain, its strain history and the presence melt during metamorphic processes (Kelsey and Hand, 2015 and references therein). In addition to annealing, different processes of recrystallization/replacement have been suggested to cause partial resetting of the U-Pb system in zircon (Schaltegger et al., 1999; Chen and Zheng, 2017), often through reaction fronts that migrate from the surface towards the centre of the grain (Fig. 1A). These processes commonly generate unbalance within the U-Pb system, via loss of Pb or gain of U, often causing discordance in the $^{207}Pb/^{235}U$ and $^{206}Pb/^{238}U$ ages. However, zircon grains that have underwent significant amounts of loss of radiogenic Pb not long after crystallization (ancient Pb-loss) can appear to be concordant, or near-concordant, due to the curvature of the concordia line in a $^{207}Pb/^{235}U$ and $^{206}Pb/^{238}U$ diagram (e.g., Andersen et al., 2019). This smearing effect can be responsible for an artificial record of protracted zircon formation. This is especially problematic in the case of zircon grains younger than the late Paleozoic Era (<ca. 400 Ma) due to low amounts of ^{207}Pb commonly generating high imprecision in the $^{207}Pb/^{235}U$ age (Bowring and Schmitz, 2003; Ireland and Williams, 2003; Spencer et al., 2016).

2.1.2. Neocrystallization of zircon during metamorphism

High temperature metamorphism can produce zircon both through subsolidus reactions (Fig. 1A and B; Möller et al., 2003) and melt crystallization/interaction in migmatites, mainly recording the cooling path (Fig. 1A and C; Kelsey, 2008; Kohn et al., 2015). Altogether, these processes can also produce a protracted zircon record (Fig. 1A). The domain effect (i.e., zircon growth in different compositional domains) can be particularly important in the timing of crystallization of heterogeneous rocks such as migmatites (e.g., Harley, 2016; Tedeschi et al., 2018; Fischer et al., 2021). In order to obtain meaningful petrological information that correlate to the temporal data (i.e., petrochronology), it is necessary to conduct studies supplementary to geochronology, such as the combination of in-situ elemental and/or isotopic geochemistry, petrography and mineral composition of inclusions from major and accessory phases, as well as other types of high-resolution imaging techniques (e.g., cathodoluminescence, atom probe tomography, X-ray compositional maps).

2.2. Zircon Lu-Hf system

Zircon is a well-known mineral for hosting high concentrations of Hf due to the high partition coefficient between zircon and other phases (e.g., garnet and apatite) in a wide range of melt composition (Fujimaki, 1986; Bea, 1996; Luo and Ayers, 2009; Nardi et al., 2013). Lu and Hf partitioning between melt and zircon plays an important role in controlling zircon isotopic characteristic and it is mainly controlled by crustal processes. Zircon grains from juvenile-like rocks are dominated by radiogenic $^{176}Hf/^{177}Hf$ resulting in suprachondritic $\varepsilon_{Hf}(t)$ signatures (i.e., $\varepsilon_{Hf}(t) > 0$), whereas zircon from crustal-like rocks are commonly derived from lower Lu/Hf sources and therefore are depleted in radiogenic $^{176}Hf/^{177}Hf$, which results in subchondritic $\varepsilon_{Hf}(t)$ (i.e., $\varepsilon_{Hf}(t) < 0$) (Bouvier et al., 2007; Vervoort and Kemp, 2016; Spencer et al., 2019). Due to its ability to record the rock source's signature and subsequent crustal processes, Lu-Hf isotopes in zircon has been widely applied to crustal evolution and detrital provenance studies (e.g., Gerdes and Zeh, 2009; Kemp et al., 2009; Collins et al., 2011; Westin

et al., 2016, 2019; Martin et al., 2020; Ribeiro et al., 2020, among many others).

Additionally, Lu-Hf isotopes in zircon can also be used to detect the existence of post-crystallization processes that may affect the zircon U-Pb system such as recent and ancient Pb loss (Vervoort and Kemp, 2016). Because $^{176}Lu/^{177}Hf$ and $^{176}Hf/^{177}Hf$ ratios evolve with time in response to crustal processes, it is expected that the $^{176}Hf/^{177}Hf$ ratio and $\varepsilon_{Hf}(t)$ signatures follow a certain crustal evolution trend such as those defined by $^{176}Lu/^{177}Hf$ between 0.010 and 0.015, commonly associated to the isotopic evolution of the average continental crust (Vervoort and Blichert-Toft, 1999; Roberts et al., 2013; Spencer et al., 2019). Therefore, deviations from this anticipated behaviour could be the result of decoupling between U-Pb and Lu-Hf systems as a response to post-crystallization disturbance, since the latter is more prone to resist geological processes such as HT-UHT metamorphism (e.g., Khondalite Belt, North China Craton; Jiao et al., 2020). This assumption is crucial for the strategies we present in the following sections.

3. Rationale: Theoretical evaluation of the effects of HT-UHT metamorphism in U-Pb zircon-based provenance investigations

The U-Pb zircon dating of metaigneous rocks is usually considered to provide a relatively simple zircon record, yielding discrete ages of crystallization and metamorphism, particularly if the rock has not been subject to anatexis (Ganade de Araujo et al., 2014; Rubatto, 2017). However, that is not the case for the zircon cores of a metaopdalite from Tedeschi et al. (2018), whose U-Pb dates spread along the concordia curve from 780 to 620 Ma (Fig. 1B, sample C8382). Tedeschi et al. (2018) interpreted such spreading in dates as reflecting disturbance of the U-Pb system, caused by the HT-UHT metamorphism. The original crystallization age of the metaopdalite was retrieved through coupled *in-situ* zircon U-Pb dating and Lu-Hf isotopes, indicating a minimum crystallization age (ca. 790 Ma). Although the zircon crystals from the metaopdalite derives of a single igneous source as demonstrated by these authors, the zircon $^{206}Pb/^{238}U$ dates spread over 160 Myr, resembling the typical distribution observed for a multisourced detrital sedimentary rock. Protracted magmatic crystallization in igneous suites could last up to 50 Myr (e.g., Jiang et al., 2016), considerably less than the 160 Myr range of dates from this metaopdalite.

Considering a simplified geological history in which the metaopdalite would be the single source of a sedimentary deposit, the resulting detrital zircon date distribution would reflect these multiple date modes. Such pattern could lead to misinterpretation of the sedimentary rock as containing multiple sources of different ages, possibly concealing its 'original' sedimentary and tectonostratigraphic settings. Furthermore, a critical issue for provenance investigations is that the original crystallization age is often considerably under-represented in the whole U-Pb age spectrum (<5% of the data, in this example; see Tedeschi et al., 2018 for details).

The following section expands on these observations and discusses the possible effects of HT-UHT metamorphism in generating artificial dates ('ages') distributions and its implications in the identification of protosources and the determination of maximum depositional ages, employing two examples of metaigneous gneisses extracted from the literature, Lewisian complex (Scotland) and Socorro-Guaxupé Nappe (Brazil).

3.1. Spurious ages spectra

Identifying the protolith of a rock that underwent HT-UHT metamorphic conditions can be challenging because of possible fluids or melt interaction, which can cause open system behaviour and a non-distinctive bulk-rock composition or typical mineral assemblage. In such cases, the U-Pb zircon data may not present reliable information towards unravelling the protolith (i.e., rocks typically containing single or multiple zircon populations) due to the smearing effect of U-Pb dates and the absence of coherent ages.

Protracted concordant zircon dates from Archean protoliths of UHT orthogneisses were described in the Brasiliano/Pan-African Socorro-Guaxupé Nappe located in southeast Brazil (analysed with Laser Ablation Inductively Coupled Plasma Mass Spectrometer – LA-ICP-MS; Tedeschi et al., 2018; Fig. 2) and in the Lewisian Complex, northwest Scotland (analysed with Secondary-ion mass spectrometry – SIMS; Whitehouse and Kemp, 2010; Fig. 3). The gneisses from the Lewisian Complex and the Socorro-Guaxupé have differences in bulk-rock composition, their zircon grains were analysed by different geochronological techniques (LA-ICP-MS vs. SIMS) and the time span between crystallization and the UHT-metamorphism is significantly different. Therefore, despite similarity in the age of the source rocks, these two examples of UHT metamorphic rocks with Archean protoliths have significant differences, which makes them ideal to test the capabilities and limitations of the strategies presented in this study. In both examples, the crystallization age was assessed by coupling CL imaging of zircon with U-Pb dating and Lu-Hf isotopes.

Because in both cases the crystallization ages were retained only by a few zircon (Whitehouse and Kemp, 2010; Tedeschi et al., 2018), the zircon grains recording the oldest dates could have been interpreted as inherited or statistical outliers (Figs. 2C, D and 3E, F). Furthermore, these UHT orthogneisses have zircon dates distribution resembling those from metasedimentary rocks, and meaningless dates modes could have been misinterpreted as detrital zircon from multiple sources of different ages (Figs. 2 and 3).

The rocks from the Lewisian Complex were crystallized at ca. 2.9 Ga (Whitehouse and Kemp, 2010; Fischer et al., 2021) and metamorphosed between 2.7 and 2.5 Ga (Taylor et al., 2020; Fischer et al., 2021), resulting in a time span of ca. 200–400 Myr between igneous crystallization and metamorphism (Fig. 3). The rocks from the Socorro-Guaxupé Nappe crystallized at ca. 2.6 Ga (Tedeschi et al., 2018) and were metamorphosed between 670 and 590 Ma (Rocha et al., 2017; 2018; Tedeschi et al., 2018; Motta et al., 2021) defining a time gap of ca. 1900–2000 Myr between crystallization and metamorphism. Prolonged suprasolidus metamorphism has been suggested between ca. 2.7–2.5 Ga for the Lewisian Complex, but no discrete tectono-metamorphic event has been described in the region in order to explain the spreading of dates between the crystallization and the onset of the metamorphism (cf., Fischer et al., 2021, for a review). Similarly, spreading of U-Pb zircon dates has been identified in the Socorro-Guaxupé Nappe between ca. 2.6–1.8 Ga, with only one tectono-metamorphic event before the UHT metamorphism at ca. 2.4 Ga suggested for the region, which could not explain the spanning of the age interval (up to 700 Myr; Fig. 2) (Tedeschi et al., 2018). Rhyacian (2300–2050 Ma) and Statherian (1800–1600 Ma) tectonic episodes have been described in SE Brazil (Heilbron et al., 2017), but no evidence that these tectonic events affected the rocks of the Socorro-Guaxupé Nappe has been found yet. The date modes identified in the probability density estimate (PDE) and Kernel density estimate (KDE) plots (Figs. 2, 5 and 6) are potentially the result of disturbance of the U-Pb system induced by the UHT metamorphic Neoproterozoic event.

The complexity in unraveling the geochronological record is remarkably enhanced if rocks showing such protracted records are eroded and fed into a sedimentary basin and/or if the protolith of the high temperature to ultrahigh temperature metamorphic rock was a multi-sourced sedimentary rock.

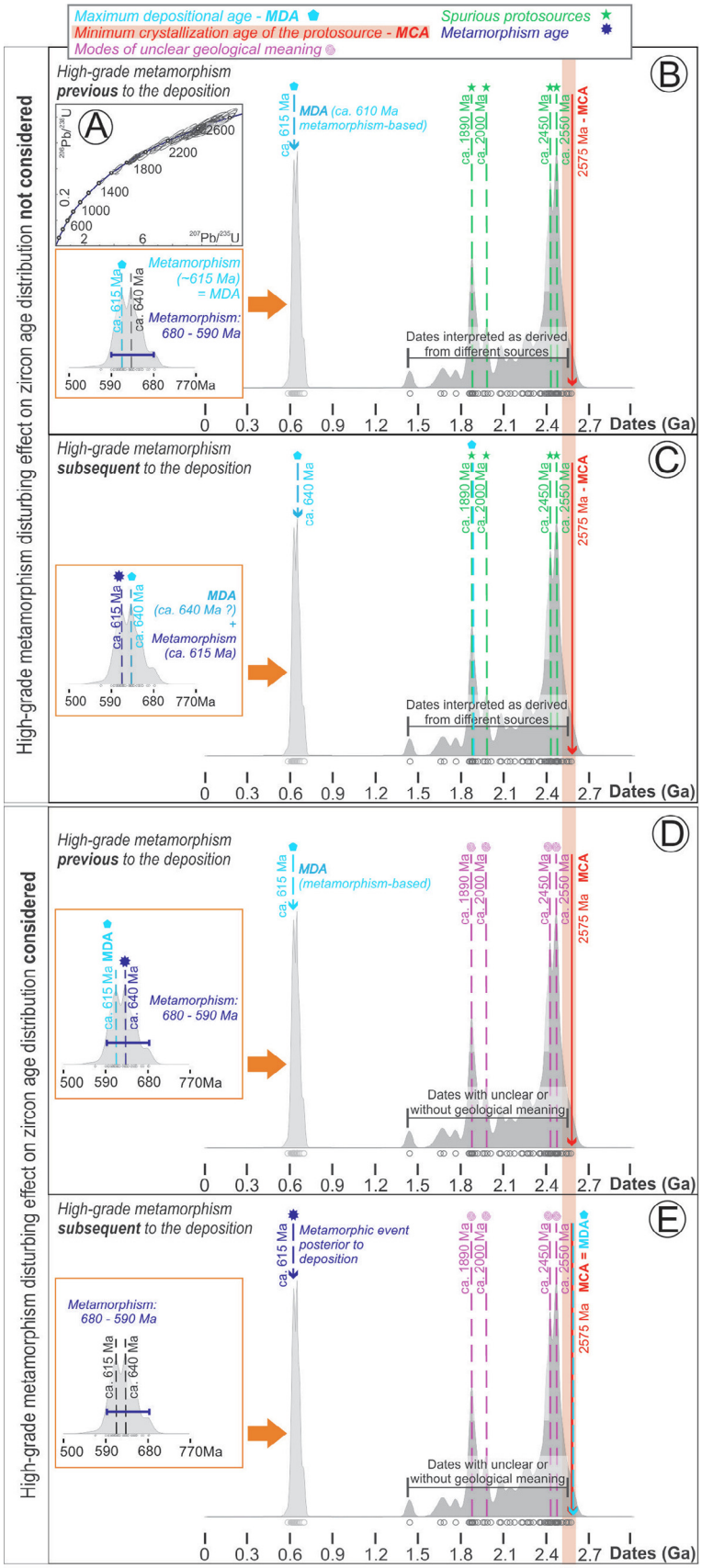
Maximum depositional age - MDA
Minimum crystallization age of the protosource - MCA
Modes of unclear geological meaning
Spurious protosources
Metamorphism age
High-grade metamorphism disturbing effect on zircon age distribution not considered
High-grade metamorphism disturbing effect on zircon age distribution considered
High-grade metamorphism previous to the deposition
High-grade metamorphism subsequent to the deposition
A
B
C
D
E
ca. 615 Ma
MDA (ca. 610 Ma metamorphism-based)
ca. 1890 Ma
ca. 2000 Ma
ca. 2450 Ma
ca. 2550 Ma
2575 Ma - MCA
Metamorphism (~615 Ma) = MDA
Metamorphism: 680 - 590 Ma
ca. 640 Ma
MDA (ca. 640 Ma ?) + Metamorphism (ca. 615 Ma)
MDA (metamorphism-based)
Metamorphic event posterior to deposition
2575 Ma MCA
MCA = MDA
Dates interpreted as derived from different sources
Dates with unclear or without geological meaning
500 590 680 770Ma
0 0.3 0.6 0.9 1.2 1.5 1.8 2.1 2.4 2.7 Dates (Ga)

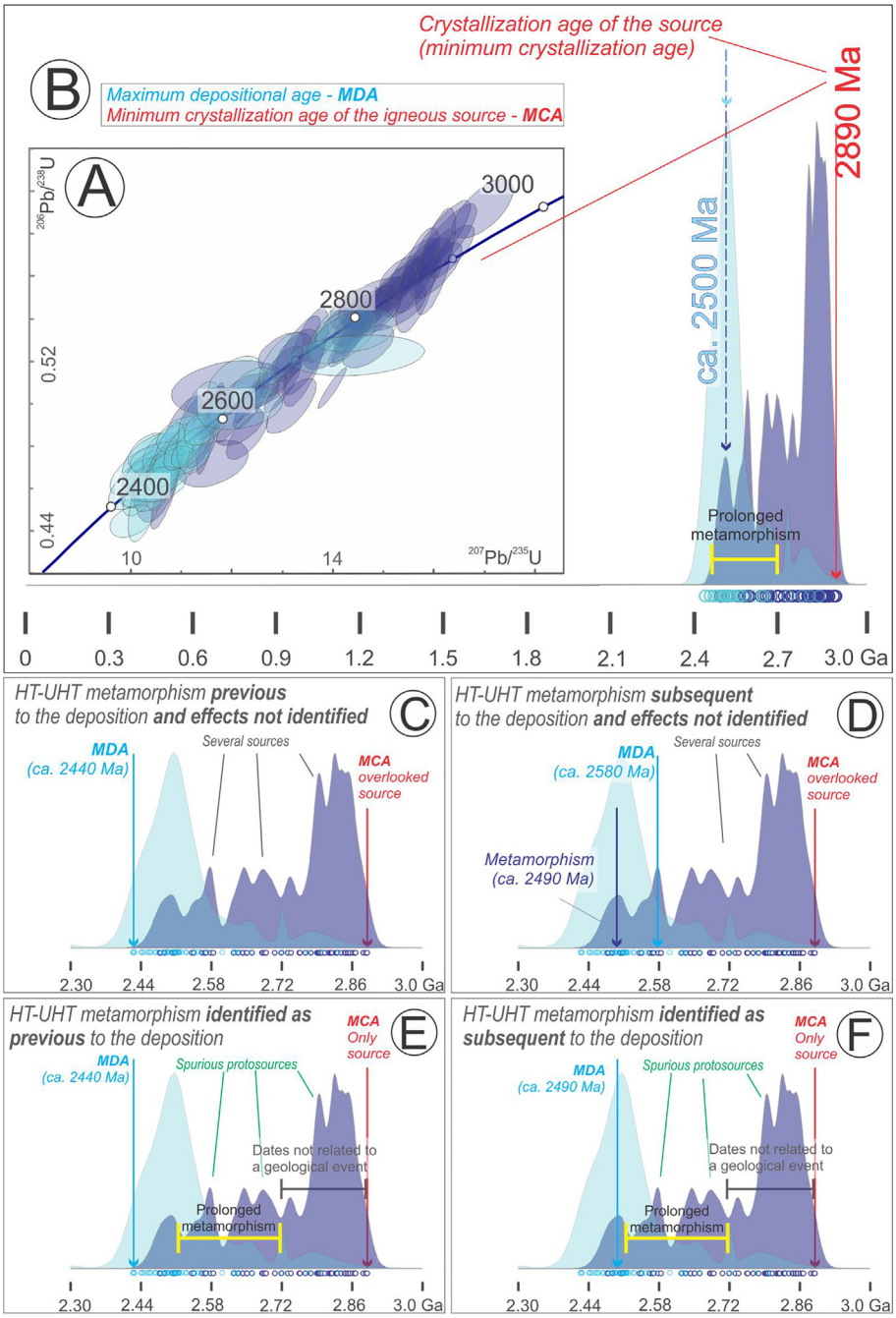

Fig. 3. Contrasting interpretations of U-Pb probability density plots of $^{207}Pb/^{206}Pb$ dates of concordant to slightly discordant zircon from a hypothetical sedimentary rock sourced from an orthogneiss from the Lewisian Complex (Mesoarchean igneous rock metamorphosed under UHT metamorphism during the Neoarchean; data from Whitehouse and Kemp, 2010), assumed as a simplified system and exhibiting a protracted geochronological record (Concordia diagram in A and probability density plot in B). Dark blue corresponds to data from cores and light blue to data from rims and newly formed grains (crystallized from the melt). The interpretations depend on whether the influence of UHT metamorphism is considered (E and F) or not (C and D), and whether the metamorphism took place before, affecting only a hypothetical source (left side; C and E), or after the sedimentation (right side; D and F). Red indicates the minimum crystallization age of the protolith (MCA), light blue indicates the hypothetical maximum depositional age (MDA) within each interpretative case; and the yellow bar represents the prolonged metamorphism identified by Taylor et al. (2020).

Fig. 2. Contrasting interpretations of U-Pb probability density plots of $^{207}Pb/^{206}Pb$ dates of nearly concordant zircon from an orthogneiss (Neoarchean igneous rock metamorphosed under UHT conditions during the Neoproterozoic; Tedeschi et al., 2018) exhibiting a protracted geochronological record (Concordia diagram presented in A) considered as a hypothetical sedimentary rock, assumed as a simplified system. In the PDP, dark grey corresponds to data from cores and light grey, rims and newly formed grains (crystallized from the melt). The interpretations depend on whether the influence of UHT metamorphism is considered/identified (spectra D and E) or not (spectra B and C), and if the metamorphism took place before, affecting only the hypothetical source (B and D), or after the sedimentation (C and E). Red indicates the minimum crystallization age of the protolith (MCA), light blue indicates the hypothetical maximum depositional age (MDA) within each interpretative case; and the orange arrow and box indicate the data from metamorphic domains.

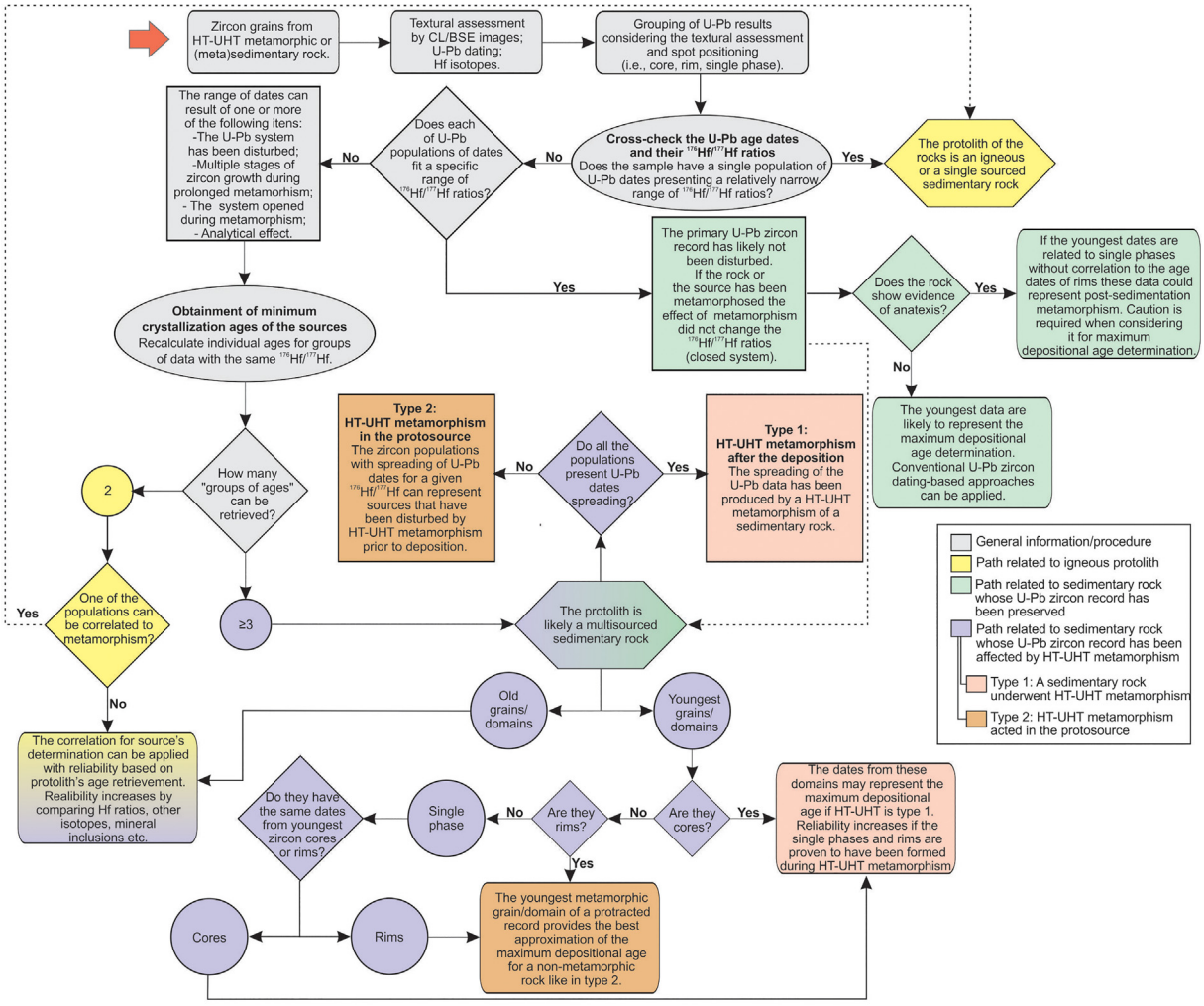

Fig. 4. Flowchart with a suggested workflow to evaluate the presence of high to ultrahigh temperature metamorphism-related bias and subsequent strategies to identify the maximum depositional age under different circumstances and their reliability. The start point of the workflow is indicated by the red arrow on the top left.

3.2. Maximum depositional age

The best approach to define the maximum depositional age in provenance studies has been a matter of debate (e.g., Dickinson and Gehrels, 2009; Spencer et al., 2016). The youngest concordant zircon grains are often used to infer the maximum depositional age (e.g., Rainbird et al., 2001), considered as recording the last event capable of disturbing the U-Pb system of zircon within the source rock, whether metamorphic, hydrothermal or magmatic.

In most of the reported HT-UHT metamorphic rocks with protracted geochronological records, the zircon dataset registers a minimum U-Pb date corresponding to the age of the last metamorphic event according to interpretations (e.g., Whitehouse and Kemp, 2010; Laurent et al., 2018). Thus, the inferred maximum depositional age based on U-Pb detrital zircon derived from the erosion of a HT-UHT metamorphic source is meaningful, since the sedimentation is subsequent to the closure of the U-Pb system within concordant zircon (Figs. 2A, C and 3C, E).

The effects on the inferred maximum depositional age are of particular concern when the HT-UHT metamorphism affects the sedimentary rock that is the object of study, rather than a rock that would be the source of a sediment. In this case the original detrital zircon dates distribution could have shifted modes that might not directly represent the geological ages recorded by the source rocks. Furthermore, the real tectono-thermal events that were experienced by the source rocks would likely be significantly underrepresented or even obliterated (Figs. 2 and 3).

These situations are presented in Figs. 2 and 3. The first scenario considers that the HT-UHT rock acted as the protosource for a sediment (Figs. 2B, D and 3C, E). Since the metamorphism can be recognized in the detrital grains as rims or newly formed grains, the maximum depositional age determination will not be affected, as it records the youngest tectono-thermal event in the area, which is prior to the deposition. When the sediment undergoes HT-UHT metamorphism the determination of MDA is likely affected. The youngest dates record the metamorphism, and the subsequent younger group can record metamorphic grains of a prolonged metamorphism (ca. 640 Ma in Fig. 2C) or of the subsequent younger peak obtained from analyses in zircon cores (ca. 1890 Ma in Fig. 2C; ca. 2580 Ma in Fig. 3D). In both cases, however, they differ significantly from the 'true' crystallization age of the rock (ca. 2575 Ma). Figs. 2D, E and 3E, F demonstrate how the age distribution can thus, be interpreted if the effects of HT-UHT metamorphism can be recognized. Nevertheless, in both cases when the HT-UHT metamorphism is not recognized, dates ('ages') modes of unclear geological meaning might affect interpretations on provenance investigations.

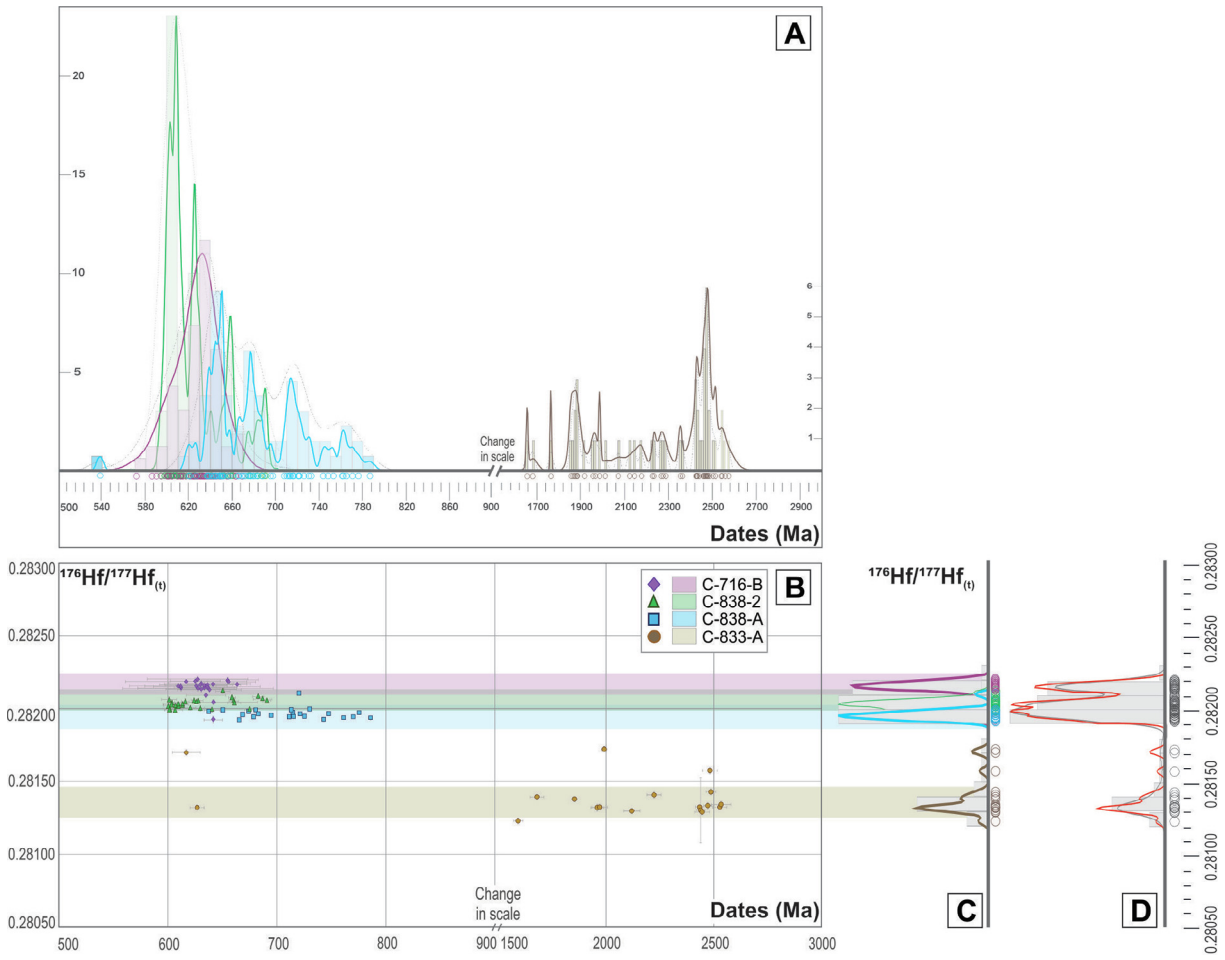

Fig. 5. Correlation between the U-Pb dates and Hf isotopic signatures of the rocks used as 'protosources' for the theoretical sediment. (A) Detrital zircon dates spectra for the four 'protosources' (vertical axes are different) with their correspondent histograms and probability density estimates curves; (B) $^{176}Hf/^{177}Hf_{(t)}$ ratio versus individual dates (t) ($^{207}Pb/^{206}Pb$ dates for grains > 1 Ga and $^{206}Pb/^{238}U$ for younger grains; errors are plotted, but can be smaller than the marker); (C, D) Probability density plots and histograms for the distribution of the apparent $^{176}Hf/^{177}Hf_{(t)}$ for the samples (C) and for the (D) the hypothetical sediment (all 'protosources' together). For sake of comparison, Kernel density estimates curves are displayed as dashed grey lines in all diagrams.

4. Strategies to avoid biases imposed by HT-UHT metamorphism in provenance studies

In order to ascertain whether a zircon population has been affected by HT-UHT metamorphism and subsequently disentangle the evolution history of a rock, one must consider several variables. We propose a flowchart to support the evaluation and identification potential bias imposed on U-Pb zircon data due to HT-UHT metamorphism (Fig. 4), and provide an approach on how to reduce or avoid it (Fig. 4).

The routinely acquisition of zircon CL and backscatter electron images and the analysis of zircon U-Pb and Lu-Hf isotopes are the primary steps to identify whether the zircon U-Pb system has been disturbed due to HT-UHT metamorphism. The identification of zircon metamorphic domains (e.g., bright luminescent rims in the CL images) cannot be solely used to assign the maximum depositional age, as they could record disturbance of the U-Pb system caused either by post- or pre-depositional metamorphism.

4.1. Protolith age determination using zircon U-Pb-Hf data

Retrieving the minimum crystallization age of protosource(s) is a fundamental step towards identifying the detrital zircon populations and therefore the provenance of the (meta)sedimentary rock. The zircon Lu-Hf system has been described to remain closed throughout several post-crystallization processes (e.g., Lenting et al., 2010; Schulz-Isenbeck et al., 2019; Barrote et al., 2020), including ultrahigh temperature metamorphism (>900 °C), unlike the U-Pb system, often resulting in decoupling from these two isotopic systems within zircon.

An estimation of the minimum crystallization age of a single population of zircon affected by later processes that result in Pb-loss is possible if the single population can be demonstrated to have homogeneous $^{176}Hf/^{177}Hf_{(t)}$. Within such a population, the oldest concordant U-Pb date can be used as a minimum crystallization age.

It is observed that zircon crystals obtained from rocks derived from a single magmatic source with little influence of magma mixing or assimilation of host rocks exhibit a well-defined $^{176}Hf/^{177}Hf_{(t)}$ signature, usually constrained inside a variation of the fourth decimal $^{176}Hf/^{177}Hf_{(t)}$ unit (0.000100) (cf., Andersen et al., 2002; Griffin et al., 2002; Andersen et al., 2004; Belousova et al., 2006). Wider variations in $^{176}Hf/^{177}Hf_{(t)}$ ratios in magmatic zircon populations can occur, with zircon crystals presenting intermediate values between "isotopic end-members". This is observed in systems affected by magma mixing or discrete populations with different $^{176}Hf/^{177}Hf_{(t)}$ ratios, as igneous rocks that underwent significant assimilation of host rocks and/or other types of xenoliths (cf., Griffin et al., 2002). It is noteworthy that different igneous sources related to a single tectonic context may also exhibit a

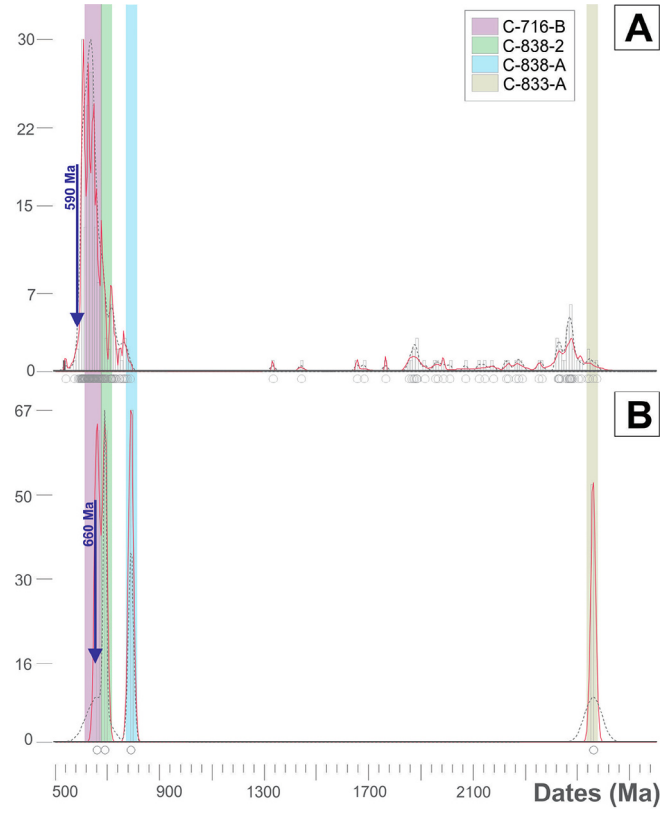

Fig. 6. Detrital zircon dates distribution for the hypothetical sediment composed of the four 'protosources' from Fig. 5. Uncorrected data presenting Pb-loss are displayed in (A) and corrected data according to distinctive Hf populations in (B). Histograms, probability density plots (in red) and Kernel density estimates curves (grey dashed lines) are displayed, together with the minimum crystallization ages of each 'protosource' represented by the correspondent coloured bands. $^{207}Pb/^{206}Pb$ dates were used for grains older than 1.0 Ga and $^{206}Pb/^{238}U$ dates for younger grains. The maximum depositional ages considered for each date distribution are indicated by the blue arrows.

well-constrained range of $^{176}Hf/^{177}Hf_{(t)}$ ratios in zircon, as observed in the Sveconorwegian-related complexes studied by Andersen et al. (2002, 2004). As a consequence, detrital zircon obtained from (meta)sedimentary rocks inserted in basins belonging to a restricted tectonic setting (as arc-related basins) also tend to come from a single source and exhibit a well constrained $^{176}Hf/^{177}Hf_{(t)}$ signature (cf. Westin et al., 2016), while multisourced basins tend to exhibit a broad variation in $^{176}Hf/^{177}Hf_{(t)}$ ratios in zircon (as observed in the detrital zircon record in Andersen et al., 2002). Based on these works, we suggest that populations of single $^{176}Hf/^{177}Hf$ comprise analyses with ratios that deviate up to the fourth decimal place of mode in probability density plots (Figs. 5 and 7). Once the populations are determined based on the Hf-isotopes, they can be treated as U-Pb-Hf populations and minimum crystallization ages can be estimated. Because igneous rocks can be multisourced (e.g., granites generated by partial melting of sediments) and can preserve inherited zircon (Boehnke et al., 2013), it is important to obtain a reliable number of U-Pb-Hf isotopic analyses that allows evaluating the role of the given modes of $^{176}Hf/^{177}Hf$ ratios distribution. Dates that do not show a clustering for Hf isotopes, are more likely to not represent the main source, but some type of contamination or inheritance and need to be evaluated accordingly.

Rocks formed in similar tectonic settings and conditions can have similar Hf isotopic signatures, although showing different ages. Such issues can be diminished by cross-checking the dates/ages and Hf isotopic signatures found in your zircon grains to those of other rocks that outcrop in the investigated area. It is important to highlight, however, that this may not be completely conclusive, as the protosource can be no longer preserved.

When the investigated rock is a migmatite and disturbance of the U-Pb system has been identified and credited to HT-UHT metamorphism, two main scenarios can be envisaged. First, if the U-Pb-Hf isotopes suggest the existence of only two zircon populations (one magmatic and one metamorphic), it is likely that the protolith is an igneous rock or, a metamorphic product of a single-sourced sedimentary rock (Fig. 4). If three or more zircon U-Pb-Hf populations can be retrieved, the protolith is likely a multi-sourced sedimentary rock. In this case, the zircon grains and specific zircon domains recording dates older than the latest metamorphic age are used to identify protosources.

The youngest population can mainly be interpreted in two ways. If the zircon dates can be distinguished into different populations by $^{176}Hf/^{177}Hf$ (Figs. 5 and 7) and all these populations display U-Pb dates that spread along the concordia curve, this record is likely the product of HT-UHT metamorphism of a sedimentary rock (type 1). Otherwise, if the spread of U-Pb dates is not observed for all unique $^{176}Hf/^{177}Hf_{(t)}$ populations, the record suggests provenance from one or more protosources that have been disturbed by HT-UHT metamorphism (or similar process capable of disturbing the U-Pb isotopic system) prior to deposition (type 2). To disclose whether the cause of the U-Pb isotopic system disturbing has been the HT-UHT metamorphism, it is necessary to find evidence of such conditions in the detrital record (see discussion below — section 4.2).

The investigation of the youngest group of zircon grains and domains has a pivotal role in evaluating the determination of the maximum depositional age. For this purpose, it is mandatory identifying the zircon CL-domains related to the HT-UHT metamorphism. For type 1 cases, the maximum depositional age of the rock might be estimated based on the oldest date from each $^{176}Hf/^{177}Hf_{(t)}$ population of cores. The maximum depositional age would be constrained by the youngest dates interpreted to be impervious to post-crystallization disturbance. For type 2 cases, the youngest metamorphic domain of a protracted record provides the best approximation of the maximum depositional age.

4.2. Identifying HT-UHT metamorphism in the detrital record

Identifying zircon grains that record HT-UHT metamorphism in the zircon population is important: (i) to consider the possibility that a protracted record can be the product of (re)crystallization during metamorphism, and; (ii) it can provide hints on whether a given population could have its U-Pb system disturbed; (iii) and assist in the correlation with potential protosources (Fig. 1). The first is particularly important in the use of the youngest population in the determination of the maximum depositional age. The second has implications in the identification of protosources based on the old zircon populations.

In type 1 rocks, where the present metamorphic rock has been subjected to HT-UHT metamorphism post deposition/crystallization, traditional *P-T* estimations via metamorphic petrology techniques would likely identify the existence of the HT-UHT conditions. However, identifying ancient HT-UHT metamorphic events that have affected the detritus in their source previously to deposition is much more difficult.

The interplay between the phases that breakdown and (re)crystallize during sub- and suprasolidus metamorphism together with the interchange of melt with host and adjacent rocks are the two main known factors controlling the Hf isotopic signature in the newly formed metamorphic zircon crystals (or domains). Considering a closed system, the absence of a Lu-Hf-host metamorphic phase (e.g., garnet) during anatexis usually lead to the maintenance of $^{176}Hf/^{177}Hf$ ratios inherited from the protolith, which

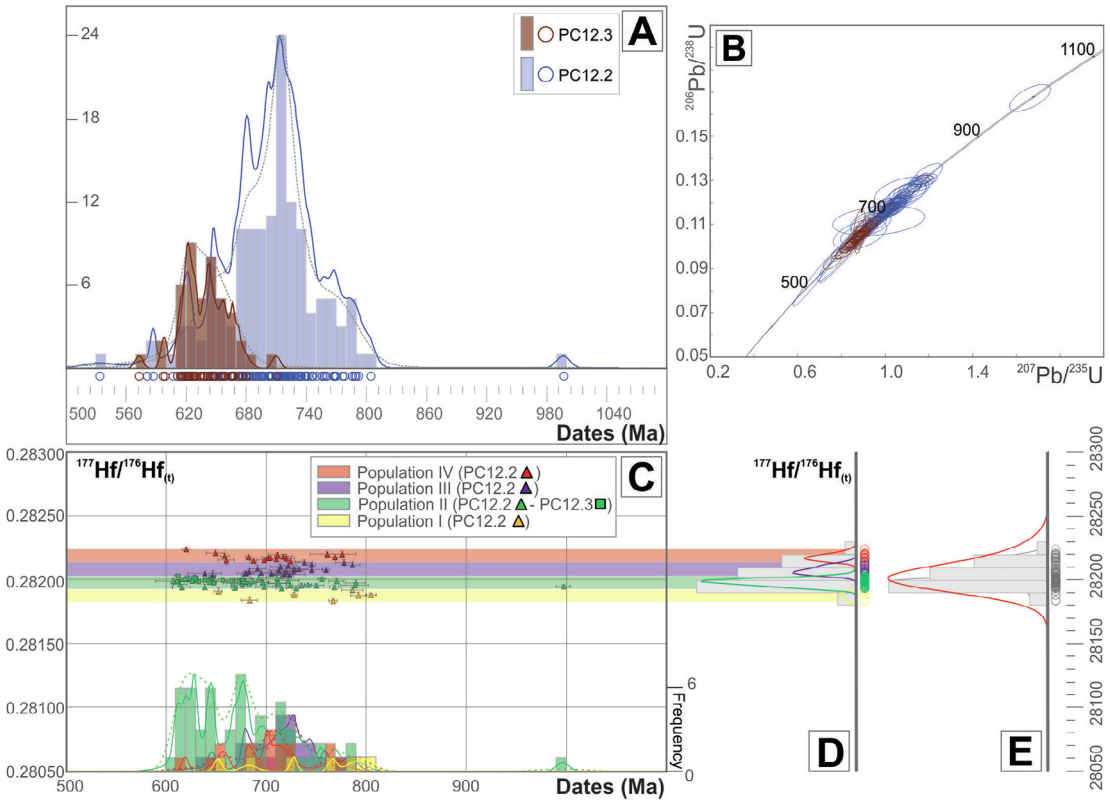

Fig. 7. Correlation between the U-Pb and Hf isotopic signatures of zircon populations in the stromatic metatexite (sample PC12.2) and the leucosome (sample PC12.3) from the migmatite. (A) Detrital zircon dates spectra for the stromatic metatexite (sample PC12.2) and leucosome (sample PC12.3) with their correspondent histograms and probability density estimate curves; (B) Concordia diagram for zircon cores from the stromatic metatexite (sample PC12.2) and leucosome (sample PC12.3); (C) $^{176}Hf/^{177}Hf_{(t)}$ ratio versus individual dates (t) ($^{206}Pb/^{238}U$ dates; errors are plotted, but can be smaller than the marker) and zircon U-Pb dates spectra for each $^{176}Hf/^{177}Hf_{(t)}$ population identified in both samples; (C, D) Probability density estimates and histograms for the distribution of the $^{176}Hf/^{177}Hf_{(t)}$ for each population (C) and (D) for the whole dataset considering samples PC12.2 and PC12.3. For sake of comparison, Kernel density estimates curves are displayed as dashed grey lines in all diagrams.

prevent the distinction of different metamorphic stages or events (Taylor et al., 2016; Rubatto, 2017; Tedeschi et al., 2018; Finch et al. 2021).

Multi-proxy approaches, including the analysis of multiple detrital minerals, (e.g., Johnson et al., 2018; Chew et al., 2020; Guo et al., 2020) can increase the successful identification of the source rocks' metamorphic history. Through thermometry-based investigations in geochronometers, such as Ti-in-zircon and Zr-in-rutile, HT-UHT conditions can be identified. There are examples in which temperatures >850 °C are recorded by the Ti-in-zircon proxy (Ewing et al., 2013; Kelsey and Hand, 2015). Cherniak and Watson (2007) have demonstrated that original Ti should be retained in zircon even under UHT conditions due to slow diffusion. However, the Ti-in-zircon thermometry on newly-grown zircon grains should be carefully evaluated, since recrystallization can produce the redistribution of Ti and that zircon more likely records the retrograde path, having crystallized during the cooling of the melt (Cherniak and Watson, 2007; Rocha et al., 2018; Motta et al., 2021). Ti-in-zircon can constitute a good approach to identify the existence of HT-UHT metamorphism, because time and temperature are constrained within the same mineral.

Furthermore, analysis of inclusions and the trace element geochemistry inventory of rutile and zircon crystals can further contribute to *P-T* determinations (e.g., Hart et al., 2016) and protolith identification (e.g., Meinhold, 2010; Grimes et al., 2015). Garnet has burgeoned as a relevant mineral in provenance studies, providing geochemical correlation with possible sources (e.g., Tolosana-Delgado et al., 2018; Schönig et al., 2021), as well as chronological data, recording lower grade metamorphic events not even registered by zircon (re)crystallization (e.g., Lu-Hf dating; Thiessen et al., 2019; Sm-Nd dating; Volante et al., 2020). In some cases, REE partitioning between phases can result in distinctive REE abundances and help correlate garnet growth and zircon crystallization during metamorphism (cf., Rubatto, 2017), which is particularly useful in identifying fingerprints of the metamorphic events. Petrochronology of monazite can also boost the deconvolution of the metamorphic evolution in high to ultrahigh temperature metamorphic rocks, due to its high closure temperature in some cases (T_c = 900–1100 °C; Cherniak et al., 2004), absence of metamictization (Barrote et al., 2020) and its correlation with garnet growth (Rocha et al., 2017).

Titanite (T_c < 650 °C; Cherniak, 1993) and apatite (T_c < 600 °C; Cherniak et al., 1991) have lower closure temperatures, but their geochemical composition can be useful in retrieving igneous sources (Bruand et al., 2017) and, combined with U-Pb dating, they may constrain the crystal cooling history during the lower temperature trajectory of the protracted metamorphism (Cioffi et al., 2019), which in turn can be useful towards determining the maximum depositional age of a rock.

5. Study cases

In this section, we employ the proposed flowchart to the investigation of two study cases involving the potential effects of HT-UHT temperature (> 850 °C) metamorphism on U-Pb zircon-based provenance studies. The examples used herein constitute HT-UHT metamorphic rocks from the Socorro-Guaxupé Nappe (SE Brazil). In the first example, we analyse the U-Pb zircon age spectra of a hypothetical sedimentary rock sourced by four known

igneous rocks subjected to ultrahigh temperature metamorphism. The Hf isotopic signatures have been used to demonstrate that the zircon grains crystallized from a single igneous source and their continuous U-Pb dates distributed along the concordia resulted from loss of radiogenic Pb (Tedeschi et al., 2018). In the second case, the flowchart is applied to the investigation of a metasedimentary migmatite whose U-Pb zircon geochronological record exhibits a continuous spreading in the concordia curve and, thus, not considering the effects of HT-UHT metamorphism may induce misleading sedimentary provenance interpretations.

5.1. Socorro-Guxupé Nappe: Geological setting

The Socorro-Guaxupé Nappe is part of a series of east-verging Nappe systems in the southern Brasília Orogen (SE Brazil). The southern Brasília Orogen was formed during the Neoproterozoic–early Palaeozoic Gondwana assembly, following the convergence and collision between the active and passive margins of the Paranapanema and São Francisco-Congo paleocontinents, respectively (Mantovani and Brito-Neves, 2005, 2009; Campos Neto et al., 2011, 2020; Trouw et al., 2013). The Socorro-Guaxupé Nappe mainly comprises granulite and amphibolite metamorphic facies rocks interpreted to record the remnants of a Neoproterozoic magmatic arc (790–640 Ma; e.g., Campos Neto and Figueiredo 1995; Vinagre et al., 2014; Rocha et al., 2018; Tedeschi et al., 2018; Motta et al., 2021), associated metasedimentary rock units (e.g., Campos Neto et al., 2011, 2020) and relicts of the Paleoproterozoic (2.1 Ga; Trouw, 2008) and Archean (2.7–2.6 Ga; Tedeschi et al., 2018) basement. Granulite and migmatite rocks from the Socorro-Guaxupé Nappe experienced UHT metamorphism with *P-T* conditions of ~900–1040 °C at 12–14 kbar (Rocha et al., 2017, 2018; Del Lama et al., 2000; Motta et al., 2021) dated at ca. 650–630 Ma (Tedeschi et al., 2018) and 630–625 Ma (Rocha et al., 2017, 2018; Motta et al., 2021). Zircon grains recording dates from ca. 630 Ma to 600 Ma have been interpreted as the transition from metamorphic peak to retrograde cooling stage (Mora et al., 2014; Rocha et al., 2017, 2018; Tedeschi et al., 2018; Motta et al., 2021), in accordance with the continental collision evolution recorded in the basement and metamafic rocks (Coelho et al., 2017; Tedeschi et al., 2017; Cioffi et al., 2019).

5.2. The hypothetical sedimentary rock sourced by UHT metamorphic rocks

The U-Pb concordant zircon data from the Socorro-Guaxupé Nappe spread along the concordia in the Wetherill diagram and are from four HT-UHT metamorphic rocks (Tedeschi et al., 2018):

(i) an orthopyroxene-clinopyroxene banded granulite from the basement (minimum crystallization age - MCA - ca. 2575 Ma; sample C833A);

(ii) a metaopdalite (ca. 790 Ma; sample C8382);

(iii) orthopyroxene-clinopyroxene banded granulite (ca. 690 Ma; sample C838A) and;

(iv) a mafic granulite enclave (ca. 660 Ma; sample C716B).

The minimum crystallization ages were retrieved by coupling zircon U-Pb and Lu-Hf isotopic data for these samples (Fig. 5). In order to simplify the investigated system, only zircon core data were considered.

5.2.1. U-Pb zircon spectrum interpretation

The diagram presented in Fig. 6A shows data uncorrected for Pb-loss from four samples, representing a theoretical sedimentary rock sourced by the erosion of the Socorro-Guaxupé UHT rocks. Eight foremost dates modes separated in two main groups can be observed. One group comprises Neoarchean (ca. 2575 Ma) to Paleoproterozoic (ca. 1440 Ma) zircon dates, with one significant mode at ca. 2480 Ma. The youngest group encloses Neoproterozoic zircon dates, spanning ca. 790–570 Ma, with seven modes at ca. 760 Ma, 715 Ma, 675 Ma, 660 Ma, 650 Ma, 630 Ma and 610 Ma.

The diagram presented in Fig. 6B displays the retrieved minimum crystallization ages based on the $^{176}Hf/^{177}Hf_{(t)}$ distribution versus U-Pb dates of the samples shown in Fig. 5B–D. In the diagram with the retrieved ages (Fig. 6B), the main modes represent the oldest dates related to a given source based on the $^{176}Hf/^{177}Hf_{(t)}$ populations, corresponding to minimum crystallization ages of ca. 2560 Ma, 790 Ma, 690 Ma and 660 Ma. The comparison between the two diagrams (Fig. 6A and B) draws attention to three main points: (i) the modes are not equivalent in both plots; (ii) the actual crystallization ages of most of the sources is underrepresented in the uncorrected diagram; and (iii) the maximum depositional ages differ in each situation.

The number of modes in both diagrams is different, furthermore, the maximum probability values and peak shapes differ. The diagram with the uncorrected data suggests contributions from sources of ca. 2.58 Ga to ca. 1.44 Ga (Fig. 6A), with the most representative contribution from a protosource crystallized at ca. 2.48 Ga. Conversely, the diagram with the Hf-corrected data (Fig. 6B) indicates that only one source crystallized at ca. 2.58 Ga contributed for pre-Neoproterozoic grains (the oldest U-Pb date for which $^{176}Hf/^{177}Hf_{(t)}$ analyses are available and indicate single zircon population). Consequently, there is a difference of at least 75 Myr between the oldest source dates that contributed to the zircon U-Pb record between the two strategies.

The same issue is observed for the younger protosources. Some dates modes record relatively similar maximum probability ages on both uncorrected (ca. 760 Ma, 675 Ma and 660 Ma) and Hf-corrected (ca. 790 Ma, 690 Ma and 660 Ma) age distribution. The modes at ca. 690 Ma and 670 Ma in the corrected age distribution are indistinguishable from the ca. 680 Ma and 660 Ma modes from the uncorrected age distribution, respectively, as their values are within analytical uncertainty (±2%–3% for laser-based methods) of each other. However, the youngest modes in the uncorrected age distribution (modes at 630 Ma and 615 Ma) cannot be correlated with verified protosources. This last observation is notably important, since the youngest age group is used to retrieve the maximum depositional age of (meta)sedimentary rocks. The maximum depositional age, considering the youngest dates without recalculation for Pb loss, is ca. 590 Ma. For the Pb loss-corrected age distribution, based on single Hf population discrimination, the maximum depositional age is represented by the youngest rock age (protosource) which is ca. 660 Ma in this hypothetical scenario.

5.2.2. Implications

The results from the hypothetical study demonstrate that provenance interpretations are significantly distinct when the data is corrected to account for the Pb-loss induced by the HT-UHT temperature metamorphism, with differences in the interpreted amount of protosources and their crystallization ages. Eight to ten protosources can potentially be identified when Pb-loss is not taken into account, whereas only four of them truly represent reliable protosources. The retrieved minimum crystallization ages based on single population from Hf-isotopic composition constitutes a more robust and reliable approach to constrain the ages of the protosources, which is key to unravel the tectonic setting in which the sediment was deposited (cf., Cawood et al., 2012). The difference in the crystallization ages for the protosources also has implications for determining the maximum depositional ages. In this example, the reliable maximum depositional age is ca. 660 Ma, differing ca. 70 Myr from the uncorrected maximum depositional age (ca. 590 Ma). Considering the tectonic setting for the evolution of the southern Brasília Orogen (cf., Trouw et al., 2013; Campos Neto et al., 2020), a 70 Myr difference could mean that

the hypothetical sediments would have been deposited either within a subduction-related setting (trench, intra or forearc basin) or later, during a continental collisional setting, such as in a foreland basin.

5.3. Para-derived HT-UHT migmatite: A natural example

The studied migmatite sample from the Socorro-Guaxupé Nappe is a metatexite composed mainly of hornblende-biotite stromatic metatexite (sample PC12.2) and leucosome (sample PC12.3). The felsic bands from the hornblende-biotite stromatic metatexite have variable amounts of plagioclase, orthoclase, quartz, biotite, hornblende and opaque minerals (ilmenite and magnetite). The mafic bands are composed of biotite, hornblende and opaque minerals (ilmenite, magnetite and sulphides), with relatively homogeneous amounts of plagioclase, orthoclase and quartz. Apatite, monazite, zircon and titanite are observed as accessory mineral phases in both bands. The leucosome has a granitic composition and is composed of plagioclase, quartz, lesser biotite and minor amounts of opaque minerals, apatite and zircon. The outcrop and microphotographies are available in the Supplementary Data 1A. The nature of the protolith (magmatic or sedimentary) cannot be interpreted based solely on petrography.

5.3.1. U-Pb zircon age distribution interpretation

Zircon grains from the stromatic metatexite and leucosome have been analysed, with the detailed description of the methods available in the Supplementary Data 1. The LA-ICP-MS U-Pb zircon analyses results are available in the Supplementary Data 2. The concordant U-Pb data of zircon cores from the stromatic metatexite (n = 138, sample PC12.2) and the leucosome (n = 44, sample PC12.3) continuously spread along the concordia in the Concordia diagram (Fig. 7B). A range of dates between ca. 805 Ma and 580 Ma is observed in the metatexite, with two outliers (ca. 995 Ma and ca. 535 Ma). A continuous distribution of concordant dates between ca. 790 Ma and 605 Ma is observed for the stromatic metatexite, and ten modes are identified in a PDE diagram at: ca. 780 Ma, 770 Ma, 760 Ma, 740 Ma, 735 Ma, 700 Ma, 715 Ma, 680 Ma, 645 Ma and 620 Ma (Fig. 7A). Four zircon populations were identified in the stromatic metatexite, based on the PDE for apparent $^{176}Hf/^{177}Hf_{(t)}$ and considering the fourth decimal place criteria, proposed herewith (Fig. 7C and D).

Population I is characterised by $^{176}Hf/^{177}Hf_{(t)}$ ratios between 0.28183 and 0.28192, with U-Pb dates between ca. 805 Ma and 650 Ma; population II has $^{176}Hf/^{177}Hf_{(t)}$ ratios between 0.28193 and 0.28203 and U-Pb dates between ca. 790 Ma and 605 Ma with one outlier dating ca. 995 Ma; population III has $^{176}Hf/^{177}Hf_{(t)}$

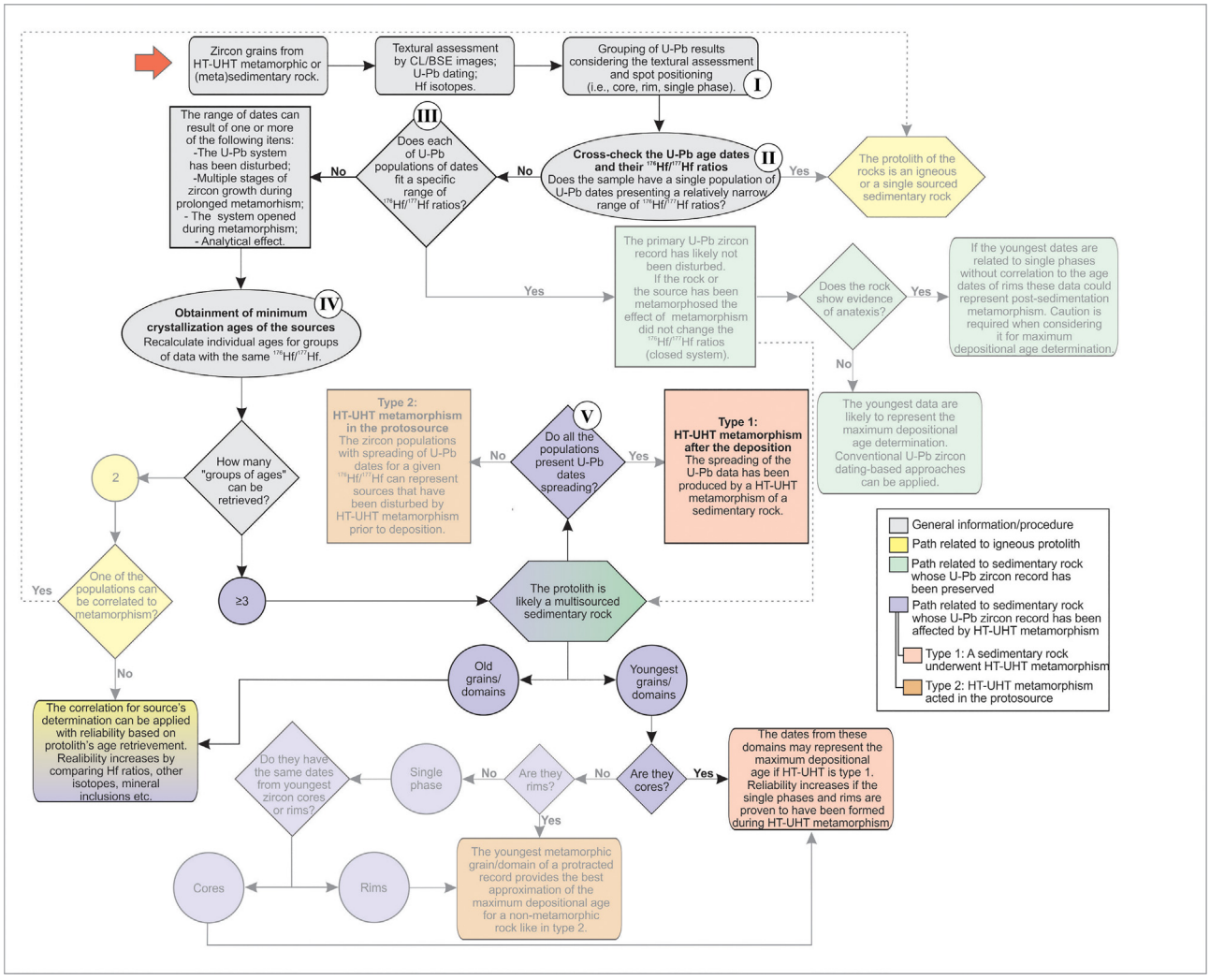

Fig. 8. Flowchart applied to the zircon dataset from the stromatic metatexite (sample PC12.2) and the leucosome (sample PC12.3), with the highlighted path corresponding to the evaluation of the natural example.

ratios between 0.28203 and 0.28213 and U-Pb dates between ca. 785 Ma and 640 Ma; and population IV has $^{176}Hf/^{177}Hf_{(t)}$ ratios between 0.28214 and 0.28224 and U-Pb dates between ca. 775 Ma and 620 Ma.

A range of dates between ca. 710 Ma and 575 Ma is observed for the grains from the leucosome, with a continuous distribution of concordant dates between ca. 680 Ma and 595 Ma. Five modes were identified in the probability density estimate diagram at ca. 670 Ma, 660 Ma, 640 Ma, 620 Ma and 600 Ma (Fig. 7A).

The $^{176}Hf/^{177}Hf_{(t)}$ (0.28197–0.28203) from the zircon cores of the leucosome (sample PC12.3) indicate a single population, with isotopic signature similar to that of population II from the stromatic metatexite (Fig. 7C).

The zircon grains of both samples were imaged via cathodoluminescence (CL), however, no systematic correlation between different textural domains and dates was observed (Step I, Fig. 8; see Supplementary Data 1C). The $^{176}Hf/^{177}Hf_{(t)}$ data indicate multiple zircon populations with a narrow range of $^{176}Hf/^{177}Hf_{(t)}$ ratios and smear of dates (Step II and III) (Fig. 7C–E). The possible explanations are (i) the zircon U-Pb system has been disturbed (e.g., Pb-loss); (ii) multiple stages of zircon growth during prolonged metamorphism; or (iii) an analytical effect (e.g., mixing of domains).

Four distinct zircon single populations were retrieved using the $^{176}Hf/^{177}Hf_{(t)}$ ratios of zircon cores (Step IV) (Fig. 7B and C), consistent with a sedimentary protolith with multiple sources. Since the zircon from the leucosome and the zircon population II from the stromatic metatexite have similar $^{176}Hf/^{177}Hf_{(t)}$, it is likely that population II records the anatectic event associated with the leucosome bands of the stromatic metatexite (see photos on the

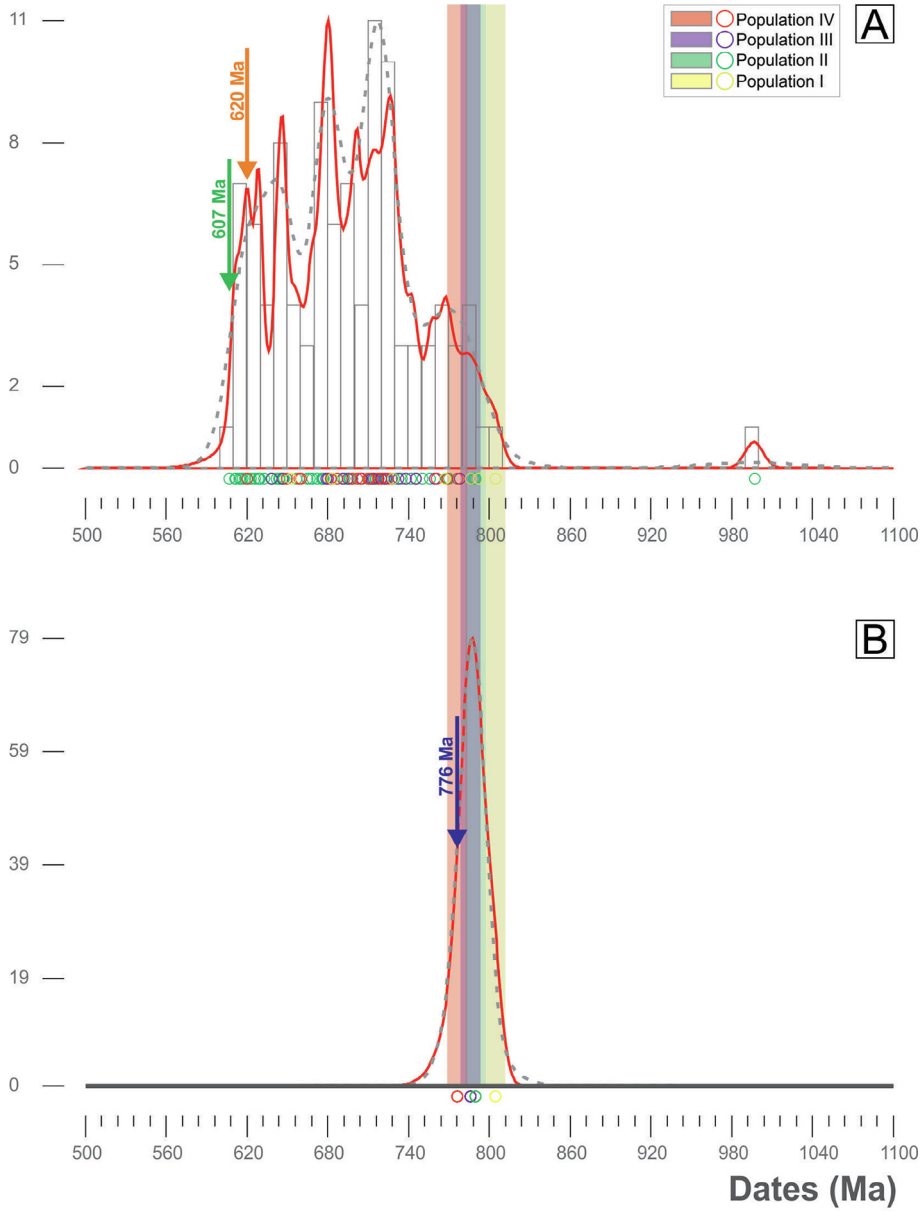

Fig. 9. U-Pb detrital zircon dates spectra for the migmatite comprising both the stromatic metatexite (PC12.2) and the leucosome (PC12.3) presented in Fig. 7A. Uncorrected data, presenting Pb-loss and possibly prolonged metamorphism are displayed in (A) and corrected data according to Hf isotopic signature in (B). Histograms, probability density estimates curves (red) and Kernel density estimates curves (grey dashed lines) are displayed. The minimum crystallization ages of each 'protosource' is represented by the correspondent coloured bands. $^{206}Pb/^{238}U$ dates were used for all grains. The maximum depositional age considered for uncorrected data (A) are indicated by the green arrow if zircon grains from Population II are considered and by the orange arrow if they are not considered (see text for discussion). The maximum depositional age for the corrected data (B) is indicated by the blue arrow.

Supplementary Data 1). Alternatively, it can also represent a different protosource. Considering that all populations present U-Pb dates spreading along the concordia (Step V, Fig. 8), we conclude that the studied rock underwent HT-UHT metamorphism after deposition (Type 1) (Fig. 8). This statement may sound obvious since the rock is a migmatite, but one can envisage alternatively a scenario in which one of the protosources was a HT-UHT rock, that then was eroded to form a sediment later metamorphosed (under conditions bellow < 850 °C). In this case, the zircon record of this rock would show the spreading of U-Pb dates only for one group of $^{176}Hf/^{177}Hf_{(t)}$ ratios, meaning that the metamorphism took place before the sedimentation of the investigated rock.

From the four zircon populations identified by the Hf isotopic data, three of them (excluding population II associated to anatexis) can be considered as representative for possible protosources of the sediments that were later metamorphosed under U(HT) metamorphic conditions. The oldest grains of each population are used as proxies for maximum depositional ages, determining the minimum crystallization ages of the protosources: ca. 804 Ma, for population I; ca. 786 Ma for population III; and ca. 776 Ma for the population IV (Fig. 9B).

5.3.2. Implications

Even though the observed distribution of zircon U-Pb dates could already suggest a metasedimentary origin for a migmatite, the smearing of dates in the concordia diagram (Fig. 7B) resembling those patterns observed for igneous protoliths that underwent metamorphism under high-temperature conditions and the non-diagnostic mineral assemblage of the stromatic metatexite hampered the determination of the protolith nature.

In a first unaware attempt, several potential sources could have been pointed out based on the PDE's U-Pb date modes identified in the two analysed samples (Fig. 7A). All those modes, however, are younger than the minimum crystallization ages retrieved for the protosources. Thus, these dates modes may have been produced as a consequence of the HT-UHT isotopic disturbance and/or new crystallization during metamorphism, and therefore the geological meanings of these modes are unclear.

The population II, comprising grains from the stromatic metatexite and the leucosome, more likely constitute the best representative of the anatexis during the metamorphic event. Thus, with the presence of at least three distinct protosources, the protolith of the migmatites was a metasedimentary rock. To disclose whether the zircon U-Pb record of this population represents prolonged metamorphism, multiple metamorphic events and/or data resetting, a petrochronological investigation would be required (likewise the proposed in section 4.2).

The minimum crystallization ages of the protosources are indistinguishable when all sources of uncertainty are considered, suggesting that the zircon grains might have originated from rocks crystallized within a narrow age interval or that these zircon do not preserve any dates that approximate that of crystallization, reflecting instead later disturbing by metamorphism and/or hydrothermalism. The first hypothesis agrees with the interpretation that the Socorro-Guaxupé Nappe host rocks from a Neoproterozoic magmatic arc and their associated sedimentary basins (e.g., Campos Neto and Figueiredo, 1995; Vinagre et al., 2014; Rocha et al., 2018; Motta et al., 2021). Regardless, the U-Pb data from the zircon cores of this sample (PC12-2) can be used to estimate maximum depositional age; however, it requires critical evaluation and Pb-loss correction to avoid underestimation. Based on the uncorrected data, two possible estimates for the maximum depositional age could be determined considering the youngest zircon core from the stromatic metatexite (sample PC12.2): ca. 605 Ma, if zircons from Population II are considered; and ca. 620 Ma, if zircon from Population II are excluded due to their $^{176}Hf/^{177}Hf_{(t)}$ ratios being the same as those found in the leucosome (Fig. 9A). Based on the corrected data, an estimated maximum depositional age of ca. 775 Ma is obtained (Fig. 9B). This implies in a ca. 155–170 Myr difference between corrected and uncorrected data.

6. Conclusions

The protracted zircon record produced during high to ultrahigh temperatures (>850 °C) metamorphism is widespread and occurred along the geological time. This study presents the HT-UHT metamorphism as a potentially significant natural phenomenon that could bias sedimentary provenance studies based on detrital zircon U-Pb analyses. In spite of the possibility of being generated by methodological and/or analytical procedures, the concordant protracted records of U-Pb zircon dates have been extensively described for HT-UHT metamorphic rocks, which strongly suggest a correlation with processes related to these extreme temperature conditions. This spread in concordant dates has been recognized regardless of the technique applied for U-Pb dating, the time span between the crystallization or deposition and the metamorphism, the composition, and the age of the rock.

The HT-UHT metamorphism can affect the detrital zircon record by (1) disturbing the U-Pb system in previously crystallized zircon which produces unreliable probability of distribution in dates, or (2) forming zircon during multiple and/or prolonged metamorphic events. Circumventing the impact of these metamorphic events on zircon records, provenance interpretation and their application in tectonic setting determinations, however, requires the identification of several variables. The first order outreach is whether the HT-UHT metamorphism affected the source of the sediment or the already deposited basin-fill strata. The maximum depositional age is less affected in the first case, as grains recording the metamorphism of the source invariably pre-date the sedimentation. In cases in which the basin-fill successions undergo HT-UHT metamorphism, their maximum depositional age might be substantially affected, inducing the formation of a spurious younger age. Remarkable variations might be also expected for the ages of older and multi-aged detrital zircon content.

To increase the success of extracting provenance information from such rocks, this study suggests a workflow to evaluate the presence of this bias and associated approaches to overcome its effects. The workflow was tested in a hypothetical sediment whose sources are metaigneous rocks concededly metamorphosed on UHT conditions, and a natural migmatite of uncertain origin and age, that also experienced HT-UHT metamorphism. In both cases spurious date modes, generated by the HT-UHT metamorphism, could have been interpreted as protosources, and caused underrepresentation of less-disturbed U-Pb zircon populations from the protosources and underestimation of maximum depositional ages which could greatly impact the interpretation of the depositional setting. These effects were minimised by the workflow proposed here and more robust age determinations were obtained from the combined U-Pb-Hf investigation, with better constraints on provenance, protosource age, maximum depositional age and, ultimately, depositional setting. Tracking the HT-UHT metamorphism in the detrital record of non-metamorphosed sediments and sedimentary rocks is more challenging however, as the protracted record can be produced by other processes. Moreover, finding the evidence of HT-UHT metamorphism in the detrital record can be not only defiant, but also a time-consuming task.

Other factors might also play crucial roles for sedimentary successions fed by temperature-disturbed zircon grains, like the geometry of the basin, sedimentary partitioning, and regimes (e.g., distance from the source, erosion rates, balance between

different types of sources). It might be especially relevant for *syn*-orogenic basins lacking volcanics and index fossils and fed by multi-aged sources. The HT-UHT metamorphism in sedimentary sources may contribute on spreading the age spectra of the analysed *syn*-orogenic strata, as well as changing the time span between the deposition and the zircon crystallization ages. Since the definition of meaningful age sources and the maximum depositional age in provenance studies based on U-Pb detrital zircon ages should rely on statistically robust data, the bias analysed here also needs to consider the statistical representativity of disturbed detrital zircon in the age spectra.

In summary, our study shows that, although HT-UHT metamorphic rocks occur in relatively small volume in the crust, not considering the effects of this type of metamorphism could lead to misinterpretation in tracking sedimentary sources, determining maximum depositional ages and analysing geodynamic settings of sedimentary basins.

Declaration of Competing Interest

The authors declare that they have no known competing financial interests or personal relationships that could have appeared to influence the work reported in this paper.

Acknowledgments

M. Tedeschi is grateful to Universidade Federal de Minas Gerais for the support during the preparation of this work. M. Tedeschi, M. Kuchenbecker, C. Lana, A.C. Pedrosa-Soares and I.A. Dussin are fellows of the Brazilian Research Council (CNPq). B. Ribeiro is financially supported by the Australian Research Council (FL160100168). Nick Roberts is thanked by his editorial handling. Erin Martin, Elizabeth Bell and two anonymous reviewers are thanked by their thorough reviews that significantly contributed to the current version of the manuscript. We thank Pierre Lanari, Kathryn Cutts and Marco A. Piacentini Pinheiro for stimulating discussions which helped to improve the manuscript.

Appendix A. Supplementary data

Supplementary data to this article can be found online at https://doi.org/10.1016/j.gsf.2022.101515.

References

Andersen, T., 2005. Detrital zircons as tracers of sedimentary provenance: limiting conditions from statistics and numerical simulation. Chem. Geol. 216, 249–270. https://doi.org/10.1016/j.chemgeo.2004.11.013.

Andersen, T., Griffin, W.L., Pearson, N.J., 2002. Crustal evolution in the SW part of the baltic shield: the Hf isotope evidence. J. Petrol. 43 (9), 1725–1747.

Andersen, T., Griffin, W.L., Jackson, S.E., Knudsen, T.-L., Pearson, N.J., 2004. Mid-Proterozoic magmatic arc evolution at the southwest margin of the Baltic Shield. Lithos 74, 289–318.

Andersen, T., Elburg, M., Magwaza, B., 2019. Sources of bias in detrital zircon geochronology: discordance, concealed lead loss and common lead correction. Earth-Sci. Rev. 197, 102899. https://doi.org/10.1016/j.earscirev.2019.102899.

Araujo, C., Pedrosa-Soares, A., Lana, C., Dussin, I., Queiroga, G., Serrano, P., Medeiros-Júnior, E., 2020. Zircon in emplacement borders of post-collisional plutons compared to country rocks: a study on morphology, internal texture, U-Th-Pb geochronology and Hf isotopes (Araçuaí orogeny, SE Brazil). Lithos 352–353, 105252.

Barham, M., Kirkland, C., Hollis, J., 2019. Spot the difference: zircon disparity tracks crustal evolution. Geology 47 (5), 435–439. https://doi.org/10.1130/G45840.1.

Barrote, V.R., McNaughton, N.J., Tessalina, S.G., Evans, N.J., Talavera, C., Zi, J.-W., McDonald, B.J., 2020. The 4D evolution of the Teutonic Bore Camp VHMS deposits, Yilgarn Craton, Western Australia. Ore Geol. Rev. 120, 103448. https://doi.org/10.1016/j.oregeorev.2020.103448.

Bea, F., 1996. Residence of REE, Y, Th and U in granites and crustal protoliths: Implications for the chemistry of crustal melts. J. Petrol. 37, 521–552.

Belousova, E.A., Kostitsyn, Y.A., Griffin, W.L., Begg, G.C., O'Reilly, S.Y., Pearson, N.J., 2010. The growth of the continental crust: Constraints from zircon Hf isotope data. Lithos 119, 457–466, 10.1016 /j.lithos.2010.07.024.

Belousova, E.A., Griffin, W.L., O'Reilly, S.Y., 2006. Zircon crystal morphology, trace element signatures and Hf isotope composition as a tool for petrogenetic modelling: examples from eastern Australian granitoids. J. Petrol. 47 (2), 329–353.

Bindeman, I.N., Melnik, O.E., 2016. Zircon survival, rebirth and recycling during crustal melting, magma crystallization, and mixing based on numerical modelling. J. Petrol. 57 (3), 437–460. https://doi.org/10.1093/petrology/egw013.

Boehnke, P., Watson, E.B.B., Trail, D., Harrison, T.M.M., Schmitt, A.K.K., 2013. Zircon saturation Re-revisited. Chem. Geol. 351, 324–334.

Bouvier, A., Vervoort, J.D., Patchett, P.J., 2007. The Lu–Hf CHUR value. Geochim. Cosmochim. Acta 71, A116.

Bowring, S.A., Schmitz, M.D., 2003 High-precision U–Pb zircon geochronology and the stratigraphic record. In: Hanchar, J.M., Hoskin, P.W.O. (Eds.), Zircon. Rev. Mineral. Geochem. 53, Washington, pp. 305-326.

Bruand, E., Fowler, M., Storey, C., Darling, J., 2017. Apatite trace element and isotope applications to petrogenesis and provenance. Amer. Mineral. 102 (1), 75–84. https://doi.org/10.2138/am-2017-5744.

Campos Neto, M.C., Figueiredo, M.C.H., 1995. The Rio Doce orogeny, southeastern Brazil. J. South Am. Earth Sci. 8 (2), 143–162.

Campos Neto, M.C., Basei, M.A.S., Janasi, V., Moraes, R., 2011. Orogen migration and tectonic setting of the Andrelândia Nappe system: an Ediacaran western Gondwana collage, south of São Francisco craton. J. South Am. Earth Sci. 32, 393–406.

Campos Neto, M.C., Cioffi, C.R., Westin, A., Rocha, B.C., Frugis, G.L., Tedeschi, M., Pinheiro, M.A.P., 2020. O Orógeno Brasília Meridional. In: Bartorelli, A., Teixeira, W., de Brito Neves, B.B. (Org.), Geocronologia e evolução tectônica do Continente Sul-Americano: a contribuição de Umberto Giuseppe Cordani. 1ed. São Paulo: Solaris Edições Culturais, 2020, v. 1, p. 146-180 (in Portuguese).

Cawood, P.A., Hawkesworth, C.J., Dhuime, B., 2012. Detrital zircon record and tectonic setting. Geology 40, 875–878. https://doi.org/10.1130/G32945.1.

Cawood, P.A., Hawkesworth, C.J., Dhuime, B., 2013. The continental record and the generation of continental crust. Geol. Soc. Am. Bull. 125, 14–32.

Chen, R.-X., Zheng, Y.-F., 2017. Metamorphic zirconology of continental subduction zone. J. Asian Earth Sci. 145, 149–176.

Cherniak, D.J., 1993. Lead diffusion in titanite and preliminary results on the effects of radiation damage on Pb transport. Chem. Geol. 110 (1–3), 177–194 http://10.1016/0009-2541(93)90253-F.

Cherniak, D.J., Watson, E.B., 2007. Ti diffusion in zircon. Chem. Geol. 242, 470–483.

Cherniak, D.J., Lanford, W.A., Ryerson, F.J., 1991. Lead diffusion in apatite and zircon using ion implantation and Rutherford backscattering techniques. Geochim. Cosmochim. Acta 55, 1663–1674. https://doi.org/10.1016/0016-7037(91)90137-T.

Cherniak, D.J., Watson, E.B., Grove, M., Harrison, T.M., 2004. Pb diffusion in monazite: a combined RBS/SIMS study. Geochim. Cosmochim. Acta 68, 829–840.

Chew, D., O'sullivan, G., Caracciolo, L., Mark, C., Tyrrell, S., 2020. Sourcing the sand: accessory mineral fertility, analytical and other biases in detrital U-Pb provenance analysis. Earth-Sci. Rev. 202, 103093. https://doi.org/10.1016/j.earscirev.2020.103093.

Chowdhury, P., Mulder, J.A., Cawood, P.A., Bhattacharjee, S., Roy, S., Wainwright, A. N., Nebel, O., Mukherjee, S., 2021. Magmatic thickening of crust in non–plate tectonic settings initiated the subaerial rise of Earth's first continents 3.3 to 3.2 billion years ago. PNAS 118 (46), e2105746118. 10.1073/pnas.2105746118.

Cioffi, C.R., Campos Neto, M.C., Möller, A., Rocha, B.C., 2019. Titanite petrochronology of the southern Brasília Orogen basement: effects of retrograde net-transfer reactions on titanite trace element compositions. Lithos 344–345, 393–408. https://doi.org/10.1016/j.lithos.2019.06.035.

Coelho, M.B., Trouw, R.A.J., Ganade, C.E., Vinagre, R., Mendes, J.C., Sato, K., 2017. Constraining timing and P-T conditions of continental collision and late overprinting in the Southern Brasília Orogen (SE-Brazil): U-Pb zircon ages and geothermobarometry of the Andrelândia Nappe System. Precambr. Res. 292, 194–215.

Collins, W.J., Belousova, E.A., Kemp, A.I.S., Murphy, J.B., 2011. Two contrasting Phanerozoic orogenic systems revealed by hafnium isotope data. Nat. Geosci. 4, 333–337. https://doi.org/10.1038/ngeo1127.

Corfu, F., Hanchar, J.M., Hoskin, P.W.O., Kinny, P., 2003. Atlas of zircon textures. In: Hanchar, J.M., Hoskin, P.W.O. (Eds.), Zircon. Rev. Mineral. Geochem. 53, Washington, pp. 469–500.

Costa, F.M., Penna, J.L.A., Martins, L.C.D., Tedeschi, M., Novo, T.A., Araujo, C.S., Rossi, P.L.V., Lana, C., Pedrosa-Soares, A.C., 2022. Zircon petrochronology reveals the moderately juvenile signature of a diatexite from the boundary zone between the Brasília and Ribeira orogens (SE Brazil): relict of a Tonian arc? J. South Am. Earth Sci. 116.

Coutts, D.S., Matthews, W.A., Hubbard, S.M., 2019. Assessment of widely used methods to derive depositional ages from detrital zircon populations. Geosci. Front. 10 (4), 1421–1435.

Del Lama, E.A., Zanardo, A., Oliveira, M.A.F., Morales, N., 2000. Exhumation of high pressure granulites of the Guaxupé complex, southeastern Brazil. Geol. J. 35, 231–249.

Dickinson, W.R., Gehrels, G.E., 2009. Use of U-Pb ages of detrital zircons to infer maximum depositional ages of strata: a test against a Colorado Plateau Mesozoic database. Earth Planet. Sci. Lett. 288, 115–125. https://doi.org/10.1016/j.epsl.2009.09.013.

Dröllner, M., Barham, M., Kirkland, C.L., Ware, B., 2021. Every zircon deserves a date: selection bias in detrital geochronology. Geol. Mag. 158, 1135–1142. 10.1017/S0016756821000145.

Ewing, T., Hermann, J., Rubatto, D., 2013. The robustness of the Zr-in-rutile and Ti-in-zircon thermometers during high-temperature metamorphism (Ivrea-Verbano Zone, northern Italy). Contrib. Mineral. Petrol. 165, 757–779. https://doi.org/10.1007/s00410-012-0834-5.

Fedo, C.M., Sircombe, K.N., Rainbird, R.H., 2003. Detrital zircon analysis of the sedimentary record. In: Hanchar, J.M., Hoskin, P.W.O. (Eds.), Zircon. Rev. Mineral. Geochem. 53, Washington, pp. 277–303.

Finch, M.A., Weinberg, R.F., Barrote, V.R., Cawood, P.A., 2021. Hf isotopic ratios in zircon reveal processes of anatexis and pluton construction. Earth Planet. Sci. Lett. 576, 117215. https://doi.org/10.1016/j.epsl.2021.117215.

Fischer, S., Prave, A.R., Johnson, T.E., Cawood, P.A., Hawkesworth, C.J., Horstwood, M. S.A., EIMF, 2021. Using zircon in mafic migmatites to disentangle complex high-grade gneiss terrains – Terrane spotting in the Lewisian complex, NW Scotland. Precambrian Res. 355, 106074. https://doi.org/10.1016/j.precamres.2020.106074.

Fornelli, A., Langone, A., Micheletti, F., Piccarreta, G., 2011. Time and duration of Variscan high-temperature metamorphic processes in the south European Variscides: constraints from U-Pb chronology and trace element chemistry of zircon. Mineral. Petrol. 103, 101–122. https://doi.org/10.1007/s0071 0-011-0156-8.

Friend, C.R.L., Kinny, P.D., 1995. New evidence for the protolith ages of Lewisian granulites, northwest Scotland. Geology 23, 1027–1030.

Fujimaki, H., 1986. Partition coefficients of Hf, Zr, and REE between zircon, apatite, and liquid. Contrib. Mineral. Petrol. 94, 42–45. https://doi.org/10.1007/BF00371224.

Ganade de Araujo, C.E., Rubatto, D., Hermann, J., Cordani, U.G., Caby, R., Basei, M.A., 2014. Ediacaran 2,500-km-long synchronous deep continental subduction in the West Gondwana Orogen. Nat. Commun. 5 (5198). https://doi.org/10.1038/ncomms6198.

Gerdes, A., Zeh, A., 2009. Zircon formation versus zircon alteration—new insights from combined U-Pb and Lu–Hf in-situ LA-ICP-MS analyses, and consequences for the interpretation of Archean zircon from the Limpopo Belt. Chem. Geol. 261, 230–243.

Griffin, W.L., Wang, X., Jackson, S.E., Pearson, N.J., O'Reilly, S.Y., Xu, X., Zhou, X., 2002. Zircon chemistry and magma mixing, SE China: In-situ analysis of Hf isotopes, Tonglu and Pingtan igneous complexes. Lithos 61, 237–269.

Grimes, C.B., Wooden, J.L., Cheadle, M.J., John, B.E., 2015. "Fingerprinting" tectono-magmatic provenance using trace elements in igneous zircon. Contrib. Mineral. Petrol. 170, 1–26.

Guo, R., Hu, X., Garzanti, E., Lai, W., Yan, B., Mark, C., 2020. How faithfully the geochronological and geochemical signatures of detrital zircon, titanite, rutile and monazite record magmatic and metamorphic events? A case study from the Himalaya and Tibet. Earth-Sci. Rev. 201, 103082. https://doi.org/10.1016/j.earscirev.2020.103082.

Harley, S.L., 2016. A matter of time: the importance of the duration of UHT metamorphism. J. Mineral. Petrol. Sci. 111, 50–72. https://doi.org/10.2465/jmps.160128.

Hart, E., Storey, C., Bruand, E., Schertl, H.-P., Alexander, B.D., 2016. Mineral inclusions in rutile: a novel recorder of HP-UHP metamorphism. Earth Planet. Sci. Lett. 446, 137–148. https://doi.org/10.1016/j.epsl.2016.04.035.

Hastie, A.R., Fitton, J.G., Bromiley, G.D., Butler, I.B., Odling, N.W.A., 2016. The origin of Earth's first continents and the onset of plate tectonics. Geology 44, 855–858. https://doi.org/10.1130/G38226.1.

Heilbron, M., Cordani, U., Alkmim, F.F., 2017. The São Francisco Craton and Its Margins. In: Heilbron, M., Cordani, U., Alkmim, F.F. (Orgs.). São Francisco Craton, Eastern Brazil Tectonic Genealogy of a Miniature Continent. Switzerland, Springer, p. 3–14.

Horstwood, M.S., Košler, J., Gehrels, G., Jackson, S.E., McLean, N.M., Paton, C., Pearson, N.J., Sircombe, K., Sylvester, P., Vermeesch, P., Bowring, J.F., Condon, D. J., Schoene, S., 2016. Community-derived standards for LA-ICP-MS U-(Th-) Pb geochronology–uncertainty propagation, age interpretation and data reporting. Geostand. Geoanal. Res. 40 (3), 311–332.

Ireland, T.R., Williams, I.S., 2003. Considerations in zircon geochronology by SIMS. In: Hanchar, J.M., Hoskin, P.W.O. (Eds.), Zircon. Rev. Mineral. Geochem. 53, Washington, pp. 215–241.

Jiang, Y.D., Schulmann, K., Sun, M., Štípská, P., Guy, A., Janoušek, V., Lexa, O., Yuan, C., 2016. Anatexis of accretionary wedge, Pacific-type magmatism, and formation of vertically stratified continental crust in the Altai Orogenic Belt. Tectonics 35, 3095–3118. https://doi.org/10.1002/2016TC004271.

Jiao, S., Guo, J., Evans, N.J., Mcdonald, B.J., Liu, P., Ouyang, D., Fitzsimons, I.C.W., 2020. The timing and duration of high-temperature to ultrahigh-temperature metamorphism constrained by zircon U–Pb–Hf and trace element signatures in the Khondalite Belt, North China Craton. Contrib. Mineral. Petrol. 175, 66. https://doi.org/10.1007/s00410-020-01706-z.

Johnson, T.E., Brown, M., Gardiner, N.J., Kirkland, C.L., Smithies, R.H., 2017. Earth's first stable continents did not form by subduction. Nature 543, 239–24, 10.1038/nature21383.

Johnson, S.P., Kirkland, C.L., Evans, N.J., McDonald, B.J., Cutten, H.N., 2018. The complexity of sediment recycling as revealed by common Pb isotopes in K-feldspar. Geosci. Front. 9, 1515–1527. https://doi.org/10.1016/j.gsf.2018.03.009.

Kelsey, D.E., 2008. On ultrahigh-temperature crustal metamorphism. Gondwana Res. 13, 1–29. https://doi.org/10.1016/j.gr.2007.06.001.

Kelsey, D.E., Hand, M., 2015. On ultrahigh temperature crustal metamorphism: phase equilibria, trace element thermometry, bulk composition, heat sources, timescales and tectonic settings. Geosci. Front. 6, 311–356. https://doi.org/10.1016/j.gsf.2014.09.006.

Kemp, A.I.S., Hawkesworth, C.J., Collins, W.J., Gray, C.M., Blevin, P.L., 2009. Isotopic evidence for rapid continental growth in an extensional accretionary orogen: the Tasmanides, eastern Australia. Earth Planet. Sci. Lett. 284, 455–466. https://doi.org/10.1016/j.epsl.2009.05.011.

Kohn, M.J., Corrie, S.L., Markley, C., 2015. The fall and rise of metamorphic zircon. Amer. Mineral. 100, 897–908. https://doi.org/10.2138/am-2015-5064.

Kuchenbecker, M., Pedrosa-Soares, A.C., Babinski, M., Reis, H.L.S., Atman, D., Costa, R. D., 2020. Towards an integrated tectonic model for the interaction between the Bambuí basin and the adjoining orogenic belts: evidences from the detrital zircon record of syn-orogenic units. J. South Am. Earth Sci. 104, 102831. https://doi.org/10.1016/j.jsames.2020.102831.

Kunz, B.E., Regis, D., Engi, M., 2018. Zircon ages in granulite facies rocks: decoupling from geochemistry above 850 °C? Contrib. Mineral. Petrol. 173, 26. https://doi.org/10.1007/s00410-018-1454-5.

Laurent, A., Bingen, B., Duchene, S., Whitehouse, M.J., Seydoux-Guillaume, A.-M., Bosse, V., 2018. Decoding a protracted zircon geochronological record in ultrahigh temperature granulite, and persistence of partial melting in the crust, Rogaland, Norway. Contrib. Mineral. Petrol. 173, 29. https://doi.org/10.1007/s00410-018-1455-4.

Lee, J., Williams, I., Ellis, D., 1997. Pb, U and Th diffusion in natural zircon. Nature 390, 159–162. https://doi.org/10.1038/36554.

Lenting, C., Geisler, T., Gerdes, A., Kooijman, E., Scherer, E.E., Zeh, A., 2010. The behavior of the Hf isotope system in radiation-damaged zircon during experimental hydrothermal alteration. Amer. Miner. 95 (8–9), 1343–1348. https://doi.org/10.2138/am.2010.3521.

Litty, C., Lanari, P., Burn, M., Schlunegger, F., 2017. Climate-controlled shifts in sediment provenance inferred from detrital zircon ages, western Peruvian Andes. Geology 45 (1), 59–62. https://doi.org/10.1130/g38371.1.

Luo, Y., Ayers, J.C., 2009. Experimental measurements of zircon/melt trace-element partition coefficients. Geochim. Cosmochim. Acta 73, 3656–3679. https://doi.org/10.1016/j.gca.2009.03.027.

Mantovani, M.S.M., Brito-Neves, B.B., 2005. The Paranapanema lithospheric block: its importance for Proterozoic (Rodinia, Gondwana) supercontinent theories. Gondwana Res. 8 (3), 303–315.

Mantovani, M.S.M., Brito-Neves, B.B., 2009. The Paranapanema Lithospheric Block: its nature and role in the Accretion of Gondwana. In: Gaucher, C., Sial, A., Halverson, G., Frimmel, H. (Eds.), Neoproterozoic-Cambrian Tectonics, Global Change and Evolution: A Focus on South Western Gondwana. Elsevier, Amsterdam, pp. 257–272.

Martin, E.L., Collins, W.J., Spencer, C.J., 2020. Laurentian origin of the Cuyania suspect terrane, western Argentina, confirmed by Hf isotopes in zircon. Bull. Geol. Soc. Am. 132, 273–290. https://doi.org/10.1130/B35150.1.

Meinhold, G., 2010. Rutile and its applications in earth sciences. Earth-Sci. Rev. 102, 1–28. https://doi.org/10.1016/j.earscirev.2010.06.001.

Mora, C.A.S., Campos Neto, M.C., Basei, M.A.S., 2014. Syn-collisional lower continental crust anataxis in the Neoproterozoic Socorro-Guaxupé Nappe System, southern Brasília Orogen, Brazil: constraints from zircon U-Pb dating, Sr-Nd-Hf signatures and whole-rock geochemistry. Precambrian Res. 255, 847–864.

Moreira, H., Lana, C., Nalini Jr., H.N., 2016. The detrital zircon record of an Archaean convergent basin in the Southern São Francisco Craton, Brazil. Precambrian Res. 275, 84–99.

Motta, R.G., Fitzsimons, I.C.W., Moraes, R., Johnson, T.T., Schuindt, S., Benetti, B.Y., 2021. Recovering P–T–t paths from ultra-high temperature (UHT) felsic orthogneiss: an example from the Southern Brasília Orogen, Brazil. Precambrian Res. 359, 106222. https://doi.org/10.1016/j.precamres.2021.106222.

Mulder, J.A., Nebel, O., Gardiner, N.J., Cawood, P.A., Wainwright, A.N., Ivanic, T.J., 2021. Crustal rejuvenation stabilised Earth's first cratons. Nat. Commun. 12, 3535. https://doi.org/10.1038/s41467-021-23805-6.

Murphy, J.B., Pisarevsky, S.A., Nance, R.D., Keppie, J.D., 2004. Neoproterozoic–early Paleozoic evolution of peri-Gondwanan terranes: implications for Laurentia-Gondwana connections. Int. J. Earth Sci. 93, 659–682. https://doi.org/10.1007/s00531-004-0412-9.

Nardi, L.V.S., Formoso, M.L.L., Müller, I.F., Fontana, E., Jarvis, K., Lamarão, C., 2013. Zircon/rock partition coefficients of REEs, Y, Th, U, Nb, and Ta in granitic rocks: Uses for provenance and mineral exploration purposes. Chem. Geol. 335, 1–7. https://doi.org/10.1016/j.chemgeo.2012.10.043.

Nelson, D.R., 2001. An assessment of the determination of depositional ages for Precambrian clastic sedimentary rocks by U-Pb dating of detrital zircons. Sediment. Geol. 141–142, 37–60.

Paula-Santos, G.M., Babinski, M., Kuchenbecker, M., Caetano-Filho, S., Trindade, R.I., Pedrosa-Soares, A.C., 2015. New evidence of an Ediacaran age for the Bambuí Group in southern São Francisco craton (eastern Brazil) from zircon U-Pb data and isotope chemostratigraphy. Gondwana Res. 28 (2), 702–720.

Pereira, I., Storey, C.D., Darling, J.R., Moreira, H., Strachan, R.A., Cawood, P.A., 2021. Detrital rutile tracks the first appearance of subduction zone low T/P paired metamorphism in the Palaeoproterozoic. Earth Planet. Sci. Lett. 570, 117069. https://doi.org/10.1016/j.epsl.2021.117069.

Rainbird, R.H., Hamilton, M.A., Young, G.M., 2001. Detrital zircon geochronology and provenance of the Torridonian, NW Scotland. Geol. Soc. London Spec. Publ. 158, 15–27.

Ribeiro, B.V., Cawood, P.A., Faleiros, F.M., Mulder, J.A., Martin, E., Finch, M.A., Raveggi, M., Teixeira, W., Cordani, U.G., Pavan, M., 2020. A long-lived active margin revealed by zircon U–Pb–Hf data from the Rio Apa Terrane (Brazil): new insights

into the Paleoproterozoic evolution of the Amazonian Craton. Precambrian Res. 350, 105919. https://doi.org/10.1016/j.precamres.2020.105919.
Roberts, N.M.W., Slagstad, T., Parrish, R.R., Norry, M.J., Marker, M., Horstwood, M.S. A., 2013. Sedimentary recycling in arc magmas: geochemical and U–Pb–Hf–O constraints on the Mesoproterozoic Suldal Arc, SW Norway. Contrib. Mineral. Petrol. 165, 507–523. https://doi.org/10.1007/s00410-012-0820-y.
Rocha, B.C., Moraes, R., Möller, A., Cioffi, C.R., Jercinovic, M.J., 2017. Timing of anatexis and melt crystallization in the Socorro-Guaxupé Nappe, SE Brazil: insights from trace element composition of zircon, monazite and garnet coupled to U-Pb geochronology. Lithos 277, 337–355.
Rocha, B.C., Moraes, R., Möller, A., Cioffi, C.R., 2018. Magmatic inheritance vs. UHT metamorphism: zircon petrochronology of granulites and petrogenesis of charnockitic leucosomes of the Socorro-Guaxupé Nappe, SE Brazil. Lithos 314–315, 16–39. https://doi.org/10.1016/j.lithos.2018.05.014.
Rubatto, D., 2002. Zircon trace element geochemistry: distribution coefficients and the link between U-Pb ages and metamorphism. Chem. Geol. 184, 123–138.
Möller, A., O'Brien, P.J., Kennedy, A., Kröner, A., 2003. Linking growth episodes of zircon and metamorphic textures to zircon chemistry: an example from the ultrahigh-temperature granulites of Rogaland (SW Norway). In: Vance, D., Müller, W., Villa, I.M., (Eds.), Geochronology: Linking the Isotopic Record with Petrology and Textures, Geol. Soc. London Spec. Publi. 220, London, pp. 65–81.
Rubatto, D., 2017. Zircon: The Metamorphic Mineral, in: Kohn, M.J., Engi, M., Lanari, P. (Eds.), Petrochronology. Rev. Mineral. Geochem. 83, Washington, pp. 261–289.
Santosh, M., Kusky, T., 2010. Origin of paired high pressure–ultrahigh-temperature orogens: a ridge subduction and slab window model. Terra Nova 22, 35–40.
Schaltegger, U., Fanning, C., Günther, D., Maurin, J.C., Schulmann, K., Gebauer, D., 1999. Growth, annealing and recrystallization of zircon and preservation of monazite in high-grade metamorphism: conventional and in-situ U-Pb isotope, cathodoluminescence and microchemical evidence. Contrib. Mineral. Petrol. 134, 186–201. https://doi.org/10.1007/s004100050478.
Schoene, B., 2014. U–Th–Pb geochronology. In: Turekian, K.K., Holland, H.D. (Eds.), Treatise on Geochemistry, The Crust. Elsevier 4, Amsterdam, pp. 341–378.
Schoene, B., Condon, D.J., Morgan, L., McLean, N., 2013. Precision and accuracy in geochronology. Elements 9, 19–24.
Schönig, J., von Eynatten, H., Tolosana-Delgado, R., and Meinhold, G.: Garnet major-element composition as an indicator of host-rock type: a machine learning approach using the random forest classifier. Contrib. Mineral. Petrol. 176, 98.
Schulz-Isenbeck, J., Bröcker, M., Berndt, J., 2019. U-Pb zircon dating of Paleozoic volcanic rocks from the Rheno-Hercynian Zone: new age constraints for the Steinkopf formation, Lahn-Dill area, Germany. Int. J. Earth Sci. 108, 1835–1855.
Seraine, M., Campos, J.E.G., Martins-Ferreira, M.A.C., Souza de Alvarenga, C.J., Chemale, F., Angelo, T.V., Spencer, C., 2021. Multi-dimensional scaling of detrital zircon geochronology constrains basin evolution of the late Mesoproterozoic Paranoá Group, central Brazil. Precambrian Res. 365, 106381.
Spencer, C.J., Kirkland, C.L., Taylor, R.J.M., 2016. Strategies towards statistically robust interpretations of in situ U-Pb zircon geochronology. Geosci. Front. 7 (4), 581–589. https://doi.org/10.1016/j.gsf.2015.11.006.
Spencer, C.J., Kirkland, C.L., Roberts, N.M.W., Evans, N.J., Liebmann, J., 2019. Strategies towards robust interpretations of in situ zircon Lu–Hf isotope analyses. Geosci. Front. 11, 843–853. https://doi.org/10.1016/j.gsf.2019.09.004.
Taylor, R.J.M., Kirkland, C.L., Clark, C., 2016. Accessories after the facts: Constraining the timing, duration and conditions of high-temperature metamorphic processes. Lithos 264, 239–257. https://doi.org/10.1016/j.lithos.2016.09.004.
Taylor, R.J.M., Johnson, T.E., Clark, C., Harrison, J.R., 2020. Persistence of melt-bearing Archean lower crust for >200 m.y.—An example from the Lewisian Complex, northwest Scotland. Geology 48 (3), 221–225. https://doi.org/10.1130/G46834.1.
Tedeschi, M., Lanari, P., Rubatto, D., Pedrosa-Soares, A., Hermann, J., Dussin, I., Pinheiro, M.A.P., Bouvier, A.-S., Baumgartner, L., 2017. Reconstruction of multiple P-T-t stages from retrogressed mafic rocks: Subduction versus collision in the Southern Brasília orogen (SE Brazil). Lithos 294–295, 283–303.
Tedeschi, M., Pedrosa-Soares, A.C., Dussin, I., Lanari, P., Novo, T., Pinheiro, M.A., Lana, C., Peters, D., 2018. Protracted zircon geochronological record of UHT garnet-free granulites in the Southern Brasília orogen (SE Brazil): petrochronological constraints on magmatism and metamorphism. Precambrian Res. 316, 101–126. https://doi.org/10.1016/j.precamres.2018.07.023.
Thiessen, E.J., Gibson, H.D., Regis, D., Pehrsson, S. J., Cutts, J. A., Smit, M.A, 2019. High-grade metamorphism flying under the radar of accessory minerals. Geology 47, 568–572. 10.1130 /G45979.1.
Tolosana-Delgado, R., von Eynatten, H., Krippner, A., Meinhold, G., 2018. A multivariate discrimination scheme of detrital garnet chemistry for use in sedimentary provenance analysis. Sediment. Geol. 375, 14–26. https://doi.org/10.1016/j.sedgeo.2017.11.003.
Trouw, R.A.J., Peternel, R., Ribeiro, A., Heilbron, M., Vinagre, R., Duffles, P., Trouw, C. C., Fontainha, M., Kussama, H.H., 2013. A new interpretation for the interference zone between the southern Brasília belt and the central Ribeira belt, SE Brazil. J. South Am. Earth Sci. 48, 43–57.
Trouw, C.C., 2008. Mapeamento da Folha Virgínia-MG, Geocronologia U-Pb (SHRIMP) em zircão e interpretação geotectônica. PhD thesis, UFRJ, Instituto de Geociências, Rio de Janeiro.
Vervoort, J.D., Blichert-Toft, J., 1999. Evolution of the depleted mantle: Hf isotope evidence from juvenile rocks through time. Geochim. Cosmochim. Acta 63, 533–556. https://doi.org/10.1016/S0016-7037(98)00274-9.
Vervoort, J.D., Kemp, A.I.S., 2016. Clarifying the zircon Hf isotope record of crust-mantle evolution. Chem. Geol. 425, 65–75. https://doi.org/10.1016/j.chemgeo.2016.01.023.
Vinagre, R., Trouw, R.A.J., Mendes, J.C., Duffles, P., Peternel, R., Matos, G., 2014. New evidence of a magmatic arc in the Southern Brasília Belt, Brazil: the Serra da Água Limpa Batholith (Socorro-Guaxupé Nappe). J. South Am. Earth Sci. 54, 120–139.
Volante, S., Pourteau, A., Collins, W.J., Blereau, E., Li, Z.-X., Smit, M., Evans, N.J., Nordsvan, A.R., Spencer, C.J., McDonald, B.J., Li, J., Gunter, C., 2020. Multiple *P–T–d–t* paths reveal the evolution of the final Nuna assembly in northeast Australia. J. Metamorphi. Geol. 38, 593–627. https://doi.org/10.1111/jmg.12532.
Wan, Y., Liu, D., Dong, C., Liu, S., Wang, S., Yang, E., 2011. U-Th–Pb behavior of zircons under high-grade metamorphic conditions: a case study of zircon dating of meta-diorite near Qixia, eastern Shandong. Geosci. Front. 2 (2), 137–146. https://doi.org/10.1016/j.gsf.2011.02.004.
Westin, A., Campos Neto, M.C., Hawkesworth, C.J., Cawood, P.A., Dhuime, B., Delavault, H., 2016. A paleoproterozoic intra-arc basin associated with a juvenile source in the Southern Brasilia Orogen: application of U-Pb and Hf-Nd isotopic analyses to provenance studies of complex areas. Precambrian Res. 276, 178–193. https://doi.org/10.1016/j.precamres.2016.02.004.
Westin, A., Campos Neto, M.C., Cawood, P.A., Hawkesworth, C.J., Dhuime, B., Delavault, H., 2019. The Neoproterozoic southern passive margin of the São Francisco craton: Insights on the pre-amalgamation of West Gondwana from U-Pb and Hf-Nd isotopes. Precambrian Res. 320, 454–471. https://doi.org/10.1016/j.precamres.2018.11.018.
Whitehouse, M., Kemp, A.I.S., 2010. On the difficulty of assigning crustal residence, magmatic protolith and metamorphic ages to Lewisian granulites: constraints from combined in situ U-Pb and Lu-Hf isotopes. Geol. Soc. London Spec. Publ. 335, 81–101.
Whitehouse, M.J., Ravindra Kumar, G.R., Rimša, A., 2014. Behaviour of radiogenic Pb in zircon during ultrahigh-temperature metamorphism: an ion imaging and ion tomography case study from the Kerala Khondalite Belt, southern India. Contrib. Mineral. Petrol. 168, 1–18.
Wisniowski, L., Pedrosa-Soares, A., Medeiros-Junior, E., Belém, J., Dussin, I., Queiroga, G., 2021. Ultra-high temperature, mid-crustal level, contact metamorphism imprinted on granulite facies paragneisses by a norite intrusion (São Gabriel da Baunilha, Araçuaí orogen, southeast Brazil). J. Metamorphi. Geol. 39, 867–895. https://doi.org/10.1111/jmg.12594.